Received: 14 April 2023 | Revised: 21 October 2023 | Accepted: 26 October 2023

DOI: 10.1111/gcb.17039

Global Change Biology WILEY

RESEARCH ARTICLE

China's conservation and restoration of coastal wetlands offset much of the reclamation-induced blue carbon losses

Bingxiong Fan | **Yangfan Li**

State Key Laboratory of Marine Environmental Science, Key Laboratory of Ministry of Education for Coastal and Wetland Ecosystems, College of the Environment and Ecology, Xiamen University, Xiamen, China

Correspondence
Yangfan Li, State Key Laboratory of Marine Environmental Science, Key Laboratory of Ministry of Education for Coastal and Wetland Ecosystems, College of the Environment and Ecology, Xiamen University, Xiamen, China.
Email: yangf@xmu.edu.cn

Funding information
National Natural Science Foundation of China Grants, Grant/Award Number: 42276232; Postdoctoral Research Foundation of China, Grant/Award Number: 2023M732933; Internal Program of State Key Laboratory of Marine Environmental Science, Grant/Award Number: MELRI2205

Abstract

China's coastal wetlands have experienced large losses and gains with rapid coastal reclamation and restoration since the end of the 20th century. However, owing to the difficulties in mapping soil organic carbon (SOC) in blue carbon stocks of coastal wetlands on a national scale, little is known about the spatial pattern of SOC stock in China's coastal wetlands and the loss and gain of SOC stock following coastal reclamation, conservation, and restoration over the past decades. Here, we developed a SOC stock map in China's coastal wetlands at 30 m spatial resolution, analyzed the spatial variability and driving factors of SOC stocks, and finally estimated SOC losses and gains due to coastal reclamation and wetland management from 1990 to 2020. We found that the total SOC stocks in China's coastal wetlands were 77.8 Tg C by 2020 with 3.6 Tg C in mangroves, 8.8 Tg C in salt marshes, and 65.4 Tg C in mudflats. Temperature, rainfall, and seawater salinity exerted the highest relative contributions to SOC spatial variability. The spatial trend of SOC density gradually decreased from south to north except for Liaoning province, with the lowest density in Shandong province. About 24.9% (19.4 Tg C) of SOC stocks in China's coastal wetlands were lost due to high-intensity reclamation, but SOC stock gained from conservation and restoration offset the reclamation-induced losses by 58.2% (11.3 Tg C) over the past three decades. These findings demonstrated the great potential of conservation and restoration of coastal wetlands in reversing the loss trend of blue carbon and contributing to the mitigation of climate change toward carbon neutrality. Our study provides significant spatial insights into the stocks, sequestration, and recovery capacity of blue carbon following rapid urbanization and management actions, which benefit the progress of global blue carbon management.

KEYWORDS
blue carbon, climate change mitigation, management, mangroves, salt marshes, soil organic carbon

1 | INTRODUCTION

Coastal wetlands are one of the global ecosystems with the largest carbon density and provide multiple ecosystem services for humans. Their carbon sink capacity is 30–50 times greater than terrestrial forests (Mcleod et al., 2011; Ouyang & Lee, 2020). The carbon pools in vegetated and unvegetated coastal wetlands, called "Blue carbon", consist of the biomass and soil carbon pools stored in mangroves, salt marshes, seagrass, and mudflats (Nellemann et al., 2009). Blue carbon plays a significant role in the ocean carbon cycle, accounting for 50% of the annual organic carbon stock in the coastal ocean, and is considered an effective and low-cost natural climate solution (Macreadie et al., 2021).

Soil organic carbon (SOC) stocks are the most important carbon pool in coastal wetlands accounting for 49%–98% of the total carbon stocks (Donato et al., 2011). Globally, the annual SOC stored in coastal wetlands is the same as that of terrestrial forests, even though coastal wetland area is only 3% of the size of terrestrial forest area (Duarte et al., 2013). However, geospatial data on SOC stocks of multiple coastal wetlands on a national scale have not yet been fully investigated. At present, remote sensing is the mainstream method to obtain the geospatial data of biomass carbon stocks on a large scale (Huang et al., 2021; Simard et al., 2019; Spawn et al., 2020), but its application to the estimation of SOC stocks has been limited due to the dense canopy of mangrove and salt marsh, covering the soil. Therefore, most studies used a simple algorithm of multiplying the mean SOC by the area to estimate the SOC stocks in coastal wetlands at national and global scales (Duarte et al., 2013; Fu et al., 2021), which caused large uncertainty, and the SOC spatial variability at finer scales cannot be captured.

Machine learning-based methods were recently applied to break the limitation of accurate estimates and the finer-scale spatial variability captured in the SOC stocks of coastal wetlands (Duarte de Paula Costa et al., 2021; Sanderman et al., 2018). Although a few studies on the estimation of carbon stocks in China's coastal wetlands have also been conducted using machine learning-based methods on a local scale, a specific type of coastal wetlands was only reported, such as salt marshes or mangroves (Li et al., 2019; Zhu et al., 2015). These studies are insufficient for understanding the spatial distribution and variability in SOC stocks across different types of coastal wetlands on a national scale. Therefore, there is an urgent need to develop maps of the SOC stocks in three types of China's coastal wetlands (mangroves, salt marshes, and mudflats), which is conducive to quantifying the spatial variability of SOC stocks and determining the conservation and restoration priority areas of coastal wetlands in China.

An estimated 63% of the global coastal wetlands have been lost since 1900 (Davidson, 2014), driven by coastal development, land cover/use conversion, pollution, overfishing, coastal erosion, and climate change (Galatowitsch, 2018; Hagger et al., 2022). The loss and degradation of coastal wetlands undermined their ability to mitigate climate change and increased CO_2 emissions through microbial decomposition, re-mineralization, and the release of carbon stored in the soil (Carnell et al., 2018; Lovelock & Reef, 2020; Salinas et al., 2020). These losses resulted in annual emissions of 0.15–1.02 million tons of CO_2 to the atmosphere (Pendleton et al., 2012). China lost 50% of coastal wetlands from 1950 to 2000, at an average rate of 24,000 ha year^{-1}, due to reclamation (Ma et al., 2014), which greatly threatens the ecosystem service of blue carbon sink and the capacity of climate change mitigation in coastal regions. The good news is a substantial increase in mangrove and salt marsh areas occurred in China since 2012, driven by increased conservation and restoration efforts (Wang et al., 2021). However, owing to the difficulties in mapping carbon stocks in coastal wetlands on a national scale, the reclamation loss and restoration gain in blue carbon in China have not been well-understood.

Here, we aim to (1) explore the spatial variability and key driving factors of SOC stocks in China's coastal wetlands; (2) clarify the blue carbon loss induced by high-intensity reclamation from 1990 to 2020; and (3) understand the benefit of China's conservation and restoration in blue carbon recovery. Therefore, we initially used a machine learning-based method to determine the driving factors of SOC stocks, and then developed a SOC stock map in China's coastal wetlands at 30 m spatial resolution to analyze the spatial variability at the estuarial, provincial, and national scales. In our study, coastal wetlands were defined to include two subgroups (vegetated tidal wetlands and mudflats), and vegetated tidal wetlands were further divided into salt marshes and mangroves (Wang et al., 2020). Finally, we estimated the losses, gains, and budget of SOC stock from 1990 to 2020 following the coastal reclamation, conservation, and restoration to reveal the benefits of China's conservation and restoration policies in the blue carbon recovery.

2 | MATERIALS AND METHODS

2.1 | SOC and accumulation datasets

We conducted a systematic review in the ISI Web of Science core database, Elsevier Scopus, Google Scholar, and China National Knowledge Infrastructure (https://www.cnki.net/). Keywords used to search the studies were "soil or sediment organic carbon," "stock," "accumulation rate," "tidal wetland or coastal wetland," "mangrove," "salt marsh," "mudflat," and "China." The following criteria were used to select publications for analysis: (1) The stocks of SOC were directly provided, or the SOC concentration (SOCC), bulk density (BD), and soil depth were provided to calculate the SOC stocks; (2) the carbon accumulation rates (CAR) were directly provided, or the SOCC and sediment accretion rate used to calculate the CAR were provided; (3) the location, longitude, and latitude of sampling sites were provided, and the core depth is greater than 20 cm. We focused only on the top meter of the soil since these pools are the most susceptible to land-use change. Since the SOC density reported in these studies is available in different soil depths, we took a published approach (Fu et al., 2021) with the depth variability of SOCC and BD across different coastal wetlands to extrapolate the SOC stocks of short cores (core depth <1 m) to 1 m, which can obtain sufficient samples and reduce subsequent modeling errors. We also compared the extrapolated SOC stocks with the true SOC stocks of the cores (1 m core depth) to evaluate the accuracy of the extrapolated SOC stocks (Figure S1). SOC stocks that were not provided in published studies were quantified by multiplying the SOCC of each layer by the BD and then adding. In total, we collected 262 SOC sampling sites and 120 CAR sampling sites in coastal wetlands of 11 coastal provinces in China (latitude from 18°N to 40°N) during 2000–2020. SOC sampling sites include 116 mangrove sites, 94 salt marsh sites, and 52 mudflat sites (Figure 1, Dataset S1). CAR sampling sites include 58 mangrove sites, 50 salt marsh sites, and 12 mudflat sites (Dataset S2).

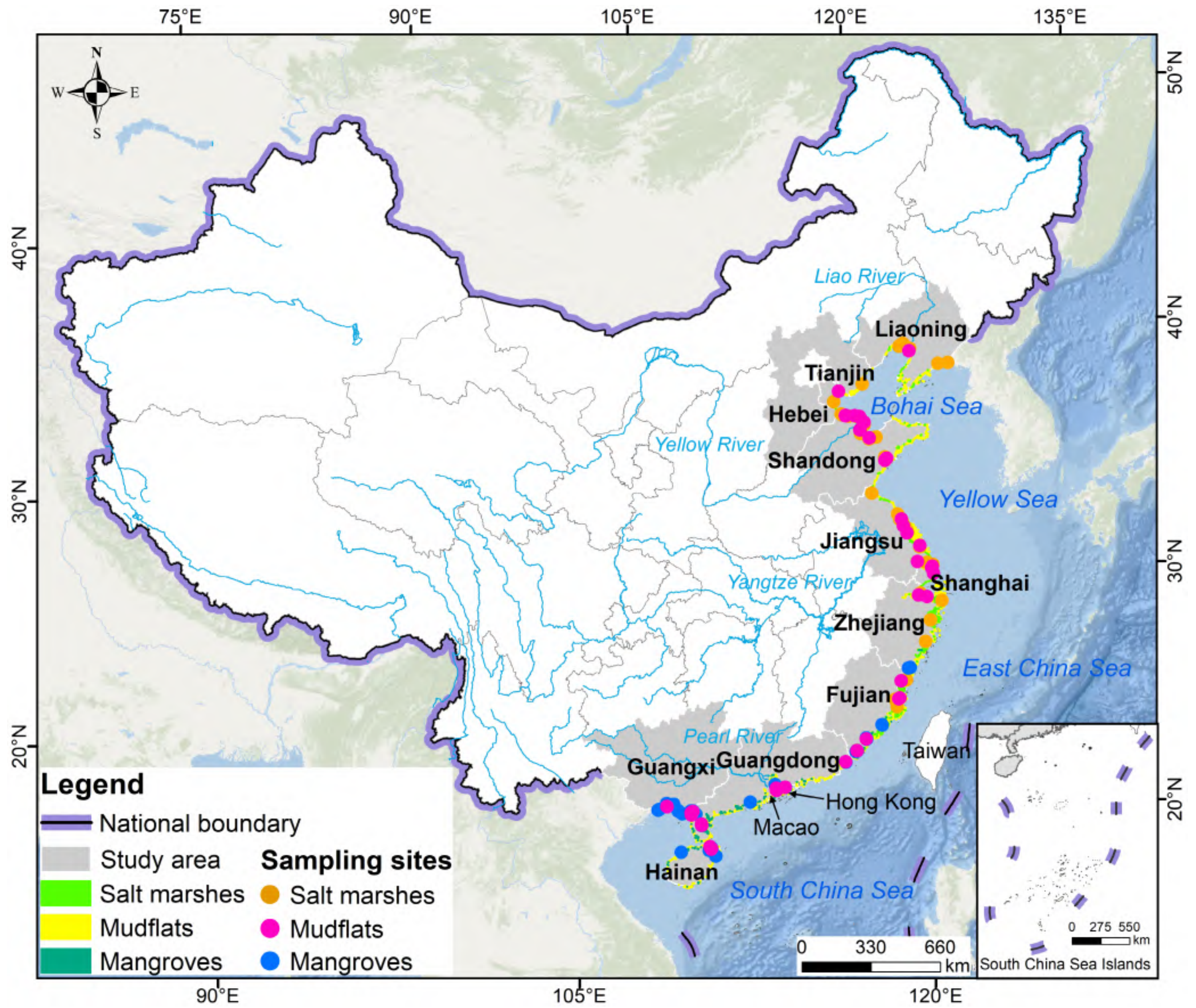

FIGURE 1 Distribution of China's coastal wetlands and SOC sampling sites. Map lines delineate study areas and do not necessarily depict accepted national boundaries.

2.2 | Coastal reclamation, conservation, and restoration data

China's coastal reclamation data from 1990 to 2020 was used to analyze the spatial loss of SOC stocks across three coastal wetlands. We collected China's coastal reclamation area and type during 1990–2015 from a published study (Sajjad et al., 2018), with over 90% of overall accuracy. Afterward, the land use/cover of the GlobeLand30 database in 2015 and 2020 was used to obtain China's coastal reclamation area during 2015–2020, which was obtained from the National Geomatics Center of China (http://www.globallandcover.com). This database was produced using more than 20,000 Landsat and Chinese HJ-1 satellite images with resolutions of 30 m, and the accuracy is up to 90% in China (Chen et al., 2017). Finally, China's coastal reclamation during 1990–2020 was developed by merging the coastal reclamation area and type during 1990–2015 and 2015–2020.

The data on conservation and restoration of coastal wetlands was used to analyze the gain of SOC stocks across three coastal wetlands over the past 30 years. The spatial extent of protected coastal wetlands was obtained by overlaying the nature reserve boundary and the extent of coastal wetlands that have persisted for the past 30 years. Conservation-driven SOC gains were then calculated over this extent. The extent of China's coastal wetlands from 1990 to 2020 was derived from remote sensing interpretation (see Section 2.3 for detailed methods). National nature reserve data for China's coastal areas were collected from the Chinese Resource and Environment Science and Data Center (https://www.resdc.cn/Default.aspx). The spatial extent of restored mangroves and salt marshes was obtained by extracting the regions where the mudflats converted into salt marshes or mangroves during 1990–2020, and these regions should be reported in the policy documents of ecological restoration from local governments. These data on restoration policies and laws were collected from published studies.

2.3 | Coastal wetlands mapping and accuracy assessment

Accurate extraction of spatial data in coastal wetlands is a critical first step in estimating and mapping SOC stocks. The coastal wetland map for 2020 was obtained from a previously published study (Zhang et al., 2022), and we only used the same method in this study to map China's coastal wetlands in 1990. We used all available Landsat 5 TM surface reflectance (SR) imagery for the year 1990 in the Google Earth Engine (GEE) cloud-processing platform. Time series of Landsat 5 TM SR imagery for the year 1990, with 6–12 months buffer prepended (18–24 months total), were collected to capture tidal variations and a full phenological cycle of vegetated wetlands. With more clouds and rain in the summer, prepended time buffers ensure sufficient cloud-free growing season observations in China. In total, 5003 images from January 1, 1990, to December 31, 1991, were available, of which 1632 scenes with cloud cover greater than 70% were filtered out, and 3371 images were ultimately collected in China's coastal zones for further analysis.

The map of China's coastal wetlands in 1990 was produced using the same classification method that integrates the tidal level and phenological features (Zhang et al., 2022). In the GEE cloud-processing platform, we first collected 12,378 georeferenced polygons as the training samples referring to multiple sources, including existing mangroves and mudflats datasets (Hu et al., 2018; Murray et al., 2019), Landsat 5 lowest tide composite images, high-resolution Google Earth images during 1990–1991. The images of the theoretical highest and lowest tide were generated by calculating a ratio of the Normalized Difference Vegetation Index and Normalized Difference Water Index, and the images of vegetation growing season and dormant season were generated by using the Near-Infrared Reflectance of vegetation (NIRv) and Plant Senescence Reflection Index (PSRI). Second, the maps of mudflats, salt marshes, and mangroves were generated by a random forest supervision classification method using the constructed training samples. Finally, we generated a validation set including 2856 random points in the GEE to assess the classification accuracy of coastal wetlands. If the validation points are located in the study area, they are assigned to four types: mangroves, salt marshes, mudflats, and others. The assessment results of classification accuracy in coastal wetlands were obtained by calculating the user's accuracy, producer's accuracy (PA), overall accuracy (OA), and F1 score (Bargiel, 2017).

2.4 | Spatial modeling of the SOC stocks in coastal wetlands

To accurately simulate the spatial distribution of SOC stocks in coastal wetlands, important biophysical and climatic environmental factors that may affect SOC stocks in China's coastal wetlands should be screened. According to the prior knowledge (Armitage & Fourqurean, 2016; Holmquist et al., 2021; Rogers, Kelleway, et al., 2019; Rogers, Saintilan, et al., 2019b; Simard et al., 2019), we selected eight climate factors including mean annual air temperature (average, minimum, and maximum), mean annual sea surface temperature (SST; average, minimum, and maximum), mean annual precipitation, mean annual solar radiation, three marine environmental factors including mean annual salinity, mean annual total suspended matter (TSM) and mean annual tidal range, five soil physicochemical factors including pH, SOC, N, P and the ratio of N and P from terrestrial ecosystems, two biological and topographic factors including canopy height and elevation (These data sources were available in Table S1), to predict the SOC stocks in mangroves, salt marshes, and mudflats. The mean value of each climate factor was first calculated based on a 30-year climatology 1990–2020, and the raster of each explanatory variable should be resampled to a unified spatial resolution (30 m) using the Nearest-Neighbor method. Then, the mean value of explanatory variables corresponding to each sampling site was extracted by the Extract by Points tool in ArcGIS 10.4 software.

There can be significant variability in the SOC stocks across three coastal wetlands, and their SOC stocks need to be modeled separately. Since there is a significant nonlinear relationship between the SOC stocks and driving factors (Figure S2), we developed three prediction models using the boosted regression tree (BRT) method in the mangroves, salt marshes, and mudflats. The BRT is a machine learning approach and ensemble method for dealing with large datasets or many variables. It is particularly robust to missing values and enhances predictive performance due to its ability to fit nonlinear relationships (Elith et al., 2008).

Before running the BRT model, the values of SOC stock need to be converted into the nearest integer to satisfy a Poisson distribution assumption, and a log-converted function was used following the gbm.step function in the dismo package of R version 3.5 software. Then, we built BRT models for mangroves, salt marshes, and mudflats with a tree complexity of 5, a learning rate of 0.001, and a bag fraction of 0.75 (75% of samples for training; Table S2). After running the BRT models of mangroves, salt marshes, and mudflats, we evaluated the model performance by 10-fold cross-validation to reduce overfitting and test the model against the remaining 25% of data. The cross-validation percent deviance explanation was calculated using the ggPerformance function within the ggBRT package (Jouffray et al., 2019), and the equation was as follows:

$$DE_{ij} = 1 - \frac{CVD_{ij}}{MTD_{ij}} \quad (1)$$

where DE_{ij} is the variance explanation of the ith model of the jth coastal wetland, CVD_{ij} is the cross-validation deviance of the ith model in the jth coastal wetland. MTD_{ij} is the mean total deviance of the ith model in the jth coastal wetland.

After evaluating the performance of multiple models, we determined the optimal prediction models for SOC stocks and identified the most important drivers for the SOC spatial variability in the mangroves, salt marshes, and mudflats, respectively. Finally, we established the spatial extrapolation models for SOC stocks in mangroves, salt marshes, and mudflats using the spatial distribution data of predictors in the model and the gbm.predict.grids function. The model was applied to simulate and predict the spatial distribution of SOC stocks in China's coastal wetlands.

2.5 | Uncertainty of the SOC stock mapping

To analyze the uncertainty in the predictive performance of our developed optimal BRTs, we ran 150 bootstrapped BRTs with 50 BRTs in mangroves, salt marshes, and mudflats, respectively, where 75% of our original data were selected by random sampling with the replacement of each time (Duarte de Paula Costa et al., 2021). These analyses were performed for each wetland on the provincial scale to improve performance efficiency. The provincial results were reassembled into a national scope for visualization and post-processing at the end of each stage. The spatial standard deviation (SD) of the predictions in each coastal wetland was finally calculated for the uncertainty analysis of SOC stocks mapping.

2.6 | Spatial analysis and accounting of the SOC loss from 1990 to 2020

Based on the developed carbon flow network from our previous study (Fan et al., 2021), we further analyzed the spatiotemporal change and drivers of SOC stocks and identified the potential natural and anthropogenic drivers (Table 1). The spatial distribution of reclamation-induced SOC loss in coastal wetlands from 1990 to 2020 was obtained by overlapping the spatial distribution of SOC stocks in coastal wetlands and coastal reclamation from 1990 to 2020.

Significant differences can exist in the influence degree of multiple drivers on SOC stocks in coastal wetlands. For the reclamation-induced and degradation-induced SOC losses, previous study indicates that soil labile organic carbon is most susceptible to ecosystem degradation and land-use change (DeGryze et al., 2004). Therefore, the amount of reclamation-induced and degradation-induced SOC loss from 1990 to 2020 in mangroves, salt marshes, and mudflats at the pixel level was estimated by multiplying the SOC stock per unit area by the SOC loss rate caused by natural degradation and different reclamation types. The equation is as follows:

$$S_{\mathrm{SOCL}} = \sum_{i=1}^{n} \mathrm{SOCS}_i \times \varepsilon \tag{2}$$

where S_{SOCL} is the amount of SOC loss, SOCS_{ij} is the SOC stock at the ith pixel, n is the number of pixels, and ε is the SOC loss rate induced by natural degradation and different reclamation types (Table S3).

2.7 | Accounting for the SOC gain from conservation and restoration

The regions where persistent coastal wetlands and natural protected areas overlaid were identified as the conservation areas of coastal wetlands. The regions where the spatial distribution of coastal wetlands in 1990 and 2020 intersected and the mudflat converted into the salt marsh or mangrove were identified as restoration areas of mangroves and salt marshes. Meanwhile, these regions should be reported in the policy documents of ecological restoration from local governments.

Sampling sites of carbon accumulation rate (CAR) in the region of coastal wetland restoration and conservation were used to estimate the amount of restoration-driven and conservation-driven SOC gain from 1990 to 2020 by multiplying the CAR per unit area by the area and times of restoration and conservation. For the restoration-driven SOC gain, if there are no CAR sampling sites in mangrove and salt marsh restoration areas, the CAR of the nearest sampling site of the same wetland type is used instead. Regarding the conservation-driven SOC gain, the CAR of mangroves, salt marshes, and mudflats were both used to calculate. The equation is as follows:

$$S_{\mathrm{SOCG}} = \mathrm{area} \times \mathrm{CAR} \times t \tag{3}$$

TABLE 1 Potential natural and anthropogenic drivers of spatiotemporal change of SOC stock in coastal wetlands.

Drivers	Ecological consequence	Impact
Construction activities	Loss in SOC stocks in coastal wetlands by converting coastal wetlands to built-up land	Negative
Aquaculture activities	Loss in SOC stocks in coastal wetlands by converting coastal wetlands to aquaculture ponds	Negative
Agriculture activities	Loss in SOC stocks in coastal wetlands by converting coastal wetlands to cropland	Negative
Salt marsh degradation	Loss in SOC stocks from salt marshes to mudflats or erosion by seawater washing	Negative
Mangrove degradation	Loss in SOC stocks from mangroves to mudflats or erosion by seawater washing	Negative
Salt marsh restoration	Increased SOC stocks in salt marshes by human intervention or natural growth	Positive
Mangrove restoration	Increased SOC stocks in mangroves by human intervention or natural growth	Positive
Conservation actions	SOC stocks gain in stable mangroves, salt marshes, and mudflats without land use/ cover conversion	Positive

where S_{SOCG} is the amount of SOC gain, area is the restoration and conservation area, CAR is the carbon accumulation rate in mangroves and salt marshes, and *t* is the time of mangrove and salt marsh restoration. The time of mangrove, salt marsh, and mudflat conservation refers to the established time of protected area. The time of mangrove and salt marsh restoration was obtained from a published study (Wang et al., 2021), which suggested the area of China's mangroves and salt marshes began to recover in 2000 and 2010, respectively. Therefore, the value of *t* for mangroves and salt marshes restoration is 20 and 10, respectively.

3 | RESULTS

3.1 | Spatial pattern of SOC stock in China's coastal wetlands

The simulated SOC density in mangroves, salt marshes, and mudflats was 166.9 ± 47.7 Mg C/ha, 86.8 ± 67.8 Mg C/ha, and 95.0 ± 51.4 Mg C/ha, respectively (Table 2), which were well-fitted to the measured values of SOC density (Figure S3). We found the SOC density in China's mangroves and salt marshes was lower than the global mean value (255 and 162 Mg C/ha, respectively; Duarte et al., 2013). We then projected the simulated SOC density across the distribution of three coastal wetlands for the year 2020, and yielded a total SOC stock estimate of 77.8 TgC for the top meter of soil using the Zonal Statistics tool in the ArcGIS 10.4 software, with 3.6 Tg C in mangroves, 8.8 Tg C in salt marshes, and 65.4 Tg C in mudflats (Table 2). The SOC stocks in mudflats, accounting for 86.1% of total SOC stocks, were the major SOC pools in China's coastal wetlands. However, its high carbon stocks have often been neglected in previous studies.

The range of SOC stocks in China's coastal wetlands was 19–310 Mg C/ha (Figure 2a–h) with 0.4–5.8 Mg C/ha of the spatial standard deviation (Figure S4). The spatial variation trend of SOC stocks was highly consistent with the trend of mean annual minimum SST and mean annual precipitation, both of which gradually decreased from south to north (Figure 2i). At the provincial scale, the highest SOC stock of coastal wetlands was in Hainan, and the lowest was in Shandong among coastal provinces (Figure 2j). At the estuarine scale, the highest SOC stock of coastal wetlands was in Dongzhai harbor (DZH), and the lowest was in the Yellow River Estuary (YRE) and Yancheng estuary cluster (YCEC) among typical estuaries (Figure 2k). In particular, the SOC stock in the Liao River Estuary

TABLE 2 SOC stocks in China's mangroves, salt marshes, and mudflats.

Coastal wetlands	Area (km^2)	SOC stock (Mg C/ha)	SD	Total SOC stocks (Tg C)
Mangroves	195.1	166.9	47.7	3.6
Salt marshes	1098.5	86.8	67.8	8.8
Mudflats	8200.3	95.0	51.4	65.4

Note: The area of coastal wetlands was derived from Zhang et al. (2022).

(LRE) was significantly higher than in the northern estuaries, which was due to the higher SOCC, rainfall, and water salinity in the LRE.

3.2 | Driving factors of SOC spatial variation in China's coastal wetlands

The final combination of variables explained 50.1%, 71.0%, and 62.4% of the deviance in SOC stocks in China's mangroves, salt marshes, and mudflats, respectively (Table S2). The optimal prediction model for mangrove SOC stocks included the mean annual minimum SST, mean annual temperature, mean annual precipitation, and mean annual solar radiation. These factors made distinctive contributions to the spatial variability of SOC, with respective percentages of 39.8%, 26.5%, 20.9%, and 13.1% (Figure 3). There are significant positive effects of mean annual minimum SST, mean annual temperature, and mean annual precipitation on the mangrove SOC stocks, but the mean annual solar radiation had significant negative effects. The optimal prediction model for salt marsh SOC stocks included the mean annual salinity, mean annual precipitation, terrestrial soil N/P, mean annual tidal range, and terrestrial SOC. These factors made distinctive contributions to the spatial variability of SOC, with respective percentages of 50.7%, 22.9%, 11.4%, 8.6%, and 6.4% (Figure 3). Mean annual salinity, mean annual precipitation, and terrestrial soil N/P had more significant effects on the salt marsh SOC stocks. The optimal prediction model for mudflat SOC stocks included the mean annual precipitation, mean annual maximum temperature, and mean annual salinity. Their relative contributions to the SOC spatial variability were 43.0%, 37.6%, and 19.4%, respectively (Figure 3). Mean annual precipitation and mean annual salinity had significant positive effects on the mudflat SOC stocks, but mean annual maximum temperature had significant negative effects.

3.3 | SOC stock losses induced by coastal reclamation

The lost wetland area induced by high-intensity coastal reclamation during 1990–2020 was 2988.7 km^2, accounting for 31.5% of the existing coastal wetlands, with the largest loss in Jiangsu province (Figure 4a). The amount of SOC stock loss due to high-intensity reclamation was 19.4 Tg C (Table S4), accounting for 24.9% of total SOC stocks and resulting in CO_2 emission of 71.2 Tg (the conversion coefficient is 3.67; Fan et al., 2021). The largest loss of SOC stocks occurred in Zhejiang, Jiangsu, and Liaoning (Figure 4b), with losses of 5.0, 3.7, and 2.8 Tg C, which together accounted for 62.2% of the total losses in SOC stock.

Aquaculture was the most important driver of SOC loss during the past 30 years (Figure 4c, Table S4), and the SOC loss induced by aquaculture activity accounted for 50% of the total SOC loss. Construction and agriculture activities accounted for 38.8% and 11.2% of the total SOC loss, respectively. However, the landscape-wide proportions of SOC loss are variable on local scales. For example, aquaculture reclamation can dominate the SOC loss in

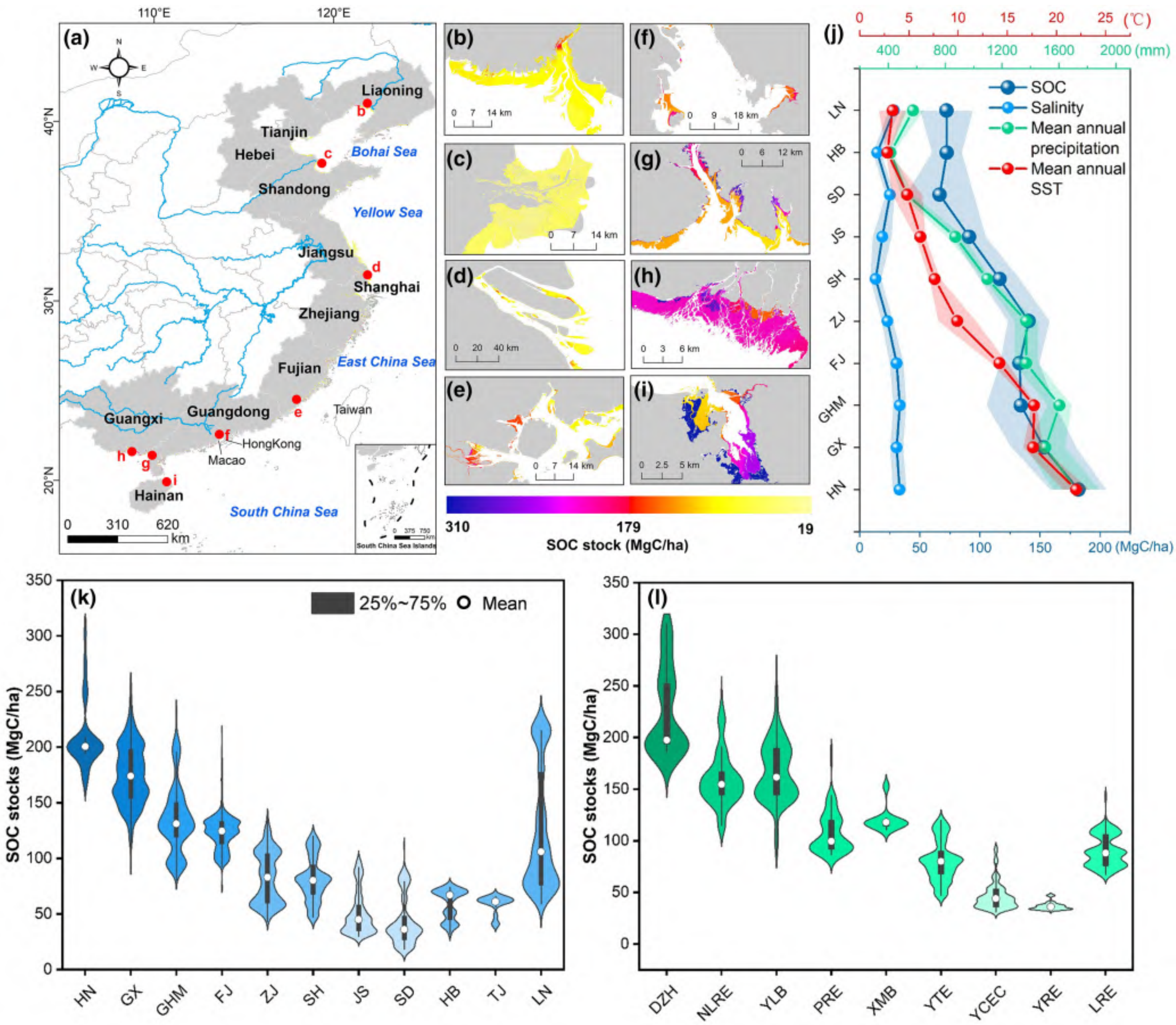

FIGURE 2 Maps and stocks of coastal wetland SOC in coastal provinces and typical estuaries. Spatial pattern of the SOC stocks in China's coastal wetlands (a). Spatial pattern of the SOC stocks in the Liao River Estuary (LRE) (b), Yellow River Estuary (YRE) (c), Yangtze Estuary (YTE) (d), Xiamen Bay (XMB) (e), Pearl River Estuary (PRE) (f), Yingluo Bay (YLB) (g), Nanliu River Estuary (NLRE) (h), and Dongzhai Harbor (DZH) (i). Characteristic of the SOC stocks and key drivers across the coastal provinces (j). SOC stock of coastal wetlands in coastal provinces was ordered latitudinally from south to north (k). SOC stock of coastal wetlands in typical estuaries was ordered latitudinally from south to north (l), YCEC is the Yancheng Estuary Cluster. Map lines delineate study areas and do not necessarily depict accepted national boundaries.

the Bohai Bay (BHB), YCEC, and Hangzhou Bay (HZB) (Figure 5a–c), accounting for 58.1%, 87.7%, and 62.9% of local total SOC loss, respectively (Table S5), and was larger than landscape-scale SOC loss (50%). SOC loss was dominated by the conversion from mudflats to aquaculture in the BHB and HZB, but 33.3% of SOC loss was induced by the salt marsh conversion in the YCEC. SOC loss is dominated by the land reclamation for construction in the BHB, Xiamen Bay (XMB), and Pearl River Estuary (PRE; Figure 5d–f), accounting for 39.6%, 81.9%, and 53.6% of local total SOC loss, respectively (Table S5), and was larger than landscape-scale SOC loss (38.8%). The conversion from mudflats to built-up land dominates the construction-induced SOC loss in these bays. Cropland reclamation can dominate SOC loss in the Yangtze Estuary (YTE) and LRE (Figure 5g,i), accounting for 60% and 39.2% of local total SOC loss, respectively (Table S5), and was much greater than landscape-scale SOC loss (11.2%). SOC loss was dominated by the conversion from mudflats to cropland in the YTE but by the salt marsh conversion in the LRE.

3.4 | SOC stock gains following conservation and restoration

The mangroves and salt marshes area in China increased by 1055.7 km^2 from 1990 to 2020 due to conservation and restoration

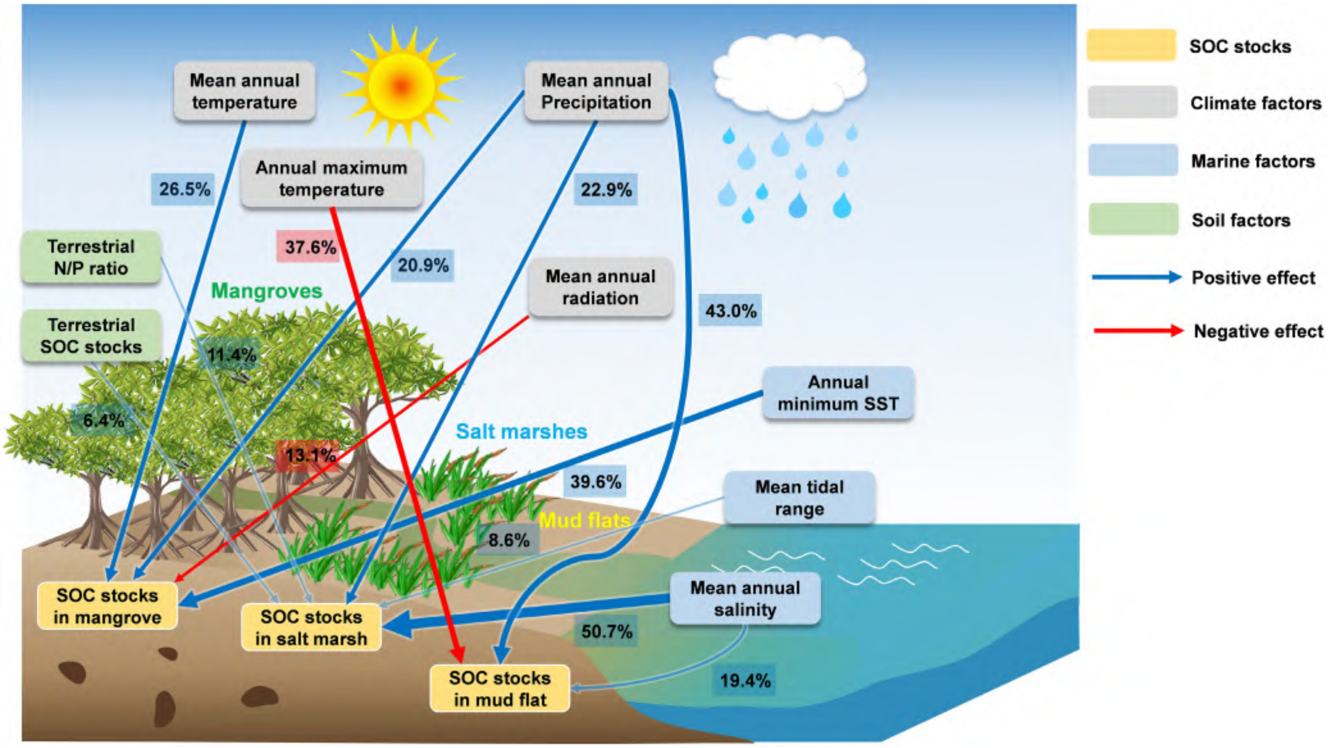

FIGURE 3 Relative contribution of driving factors on the SOC stocks in China's mangroves, salt marshes, and mudflats. The blue arrows represent the positive effects, and the red arrows represent the negative ones. The numbers in rectangular are the relative contribution.

(Table S6), with the largest gain in Jiangsu province (Figure 4b). The increased SOC stocks driven by conservation and restoration of coastal wetlands were 11.3 Tg C (Table S4) and can offset the reclamation-induced SOC losses by 58.2%. On the provincial scale, the large gain of SOC stocks occurred in Jiangsu, Shandong, and Liaoning, with gains of 2.6, 2.5, and 1.8 Tg C, which together accounted for 61.2% of the total gains in SOC stocks. However, the large SOC losses and little recovery resulted in a great deficit of SOC pools in Zhejiang and Hebei (Figure 4b). It suggested that more restoration efforts are needed to recover the SOC stock in these provinces.

Coastal wetland conservation was the most important driver of SOC gain during the past 30 years, and the conservation-driven SOC gain accounted for 75.4% of the total SOC gains (Figure 4c, Table S4). On the provincial scale, the conservation-driven SOC gain mainly occurred in Shandong, Jiangsu, and Liaoning, which was 2.1 Tg C, 2.0 Tg C, and 1.8 Tg C, respectively. The restoration-driven SOC gain in mangroves mainly occurred in Guangxi (YLB, NLRE, and QRE), which was 0.2 Tg C (Figure 6, Table S4). The restoration-driven SOC gain in salt marshes mainly occurred in Jiangsu (YCEC), which was 0.6 Tg C (Figure 6, Table S4). On the estuarial scale, owing to the extensive salt marsh restoration and mudflat conservation, the SOC gain mainly occurred in YRE of Shandong, LRE of Liaoning, and YCEC of Jiangsu, which was 1.9 Tg C, 1.2 Tg C, and 0.9 Tg C, respectively (Figure 6) and together accounted for 35.7% of the total SOC gains.

3.5 | Net change in SOC stock of China's coastal wetland

The coastal wetland area in 1990 and 2020 was 11,800.7 and 9493.9 km^2, respectively, with an overall accuracy of 96.9% and 97.1% (Table S7). The net loss area of China's coastal wetlands was 2306.7 km^2 from 1990 to 2020 (Table 3), with 80% losses from the mudflats. The net change in SOC stock due to landscape changes in coastal wetlands during 1990–2020 was −8.1 Tg C (net loss) in China (Table 3), with the largest net loss in SOC stock in Zhejiang (−4.0 Tg C) and the largest net gain in Shangdong (1.1 Tg C). Shangdong and Fujian displayed a net loss in wetland area, but a net gain in SOC stock (Table 3). Shanghai and Hainan presented a net gain in wetland area, but a net loss in SOC stock.

4 | DISCUSSION

4.1 | A 30 m spatial resolution map of SOC stocks in China's coastal wetlands

Developing a fine resolution map of SOC stocks and understanding the spatial variability and driving factors of SOC stocks in China's coastal wetlands were key data support for formulating the conservation and restoration of coastal wetlands. Although a map of global mangrove SOC stocks at 30 m spatial resolution

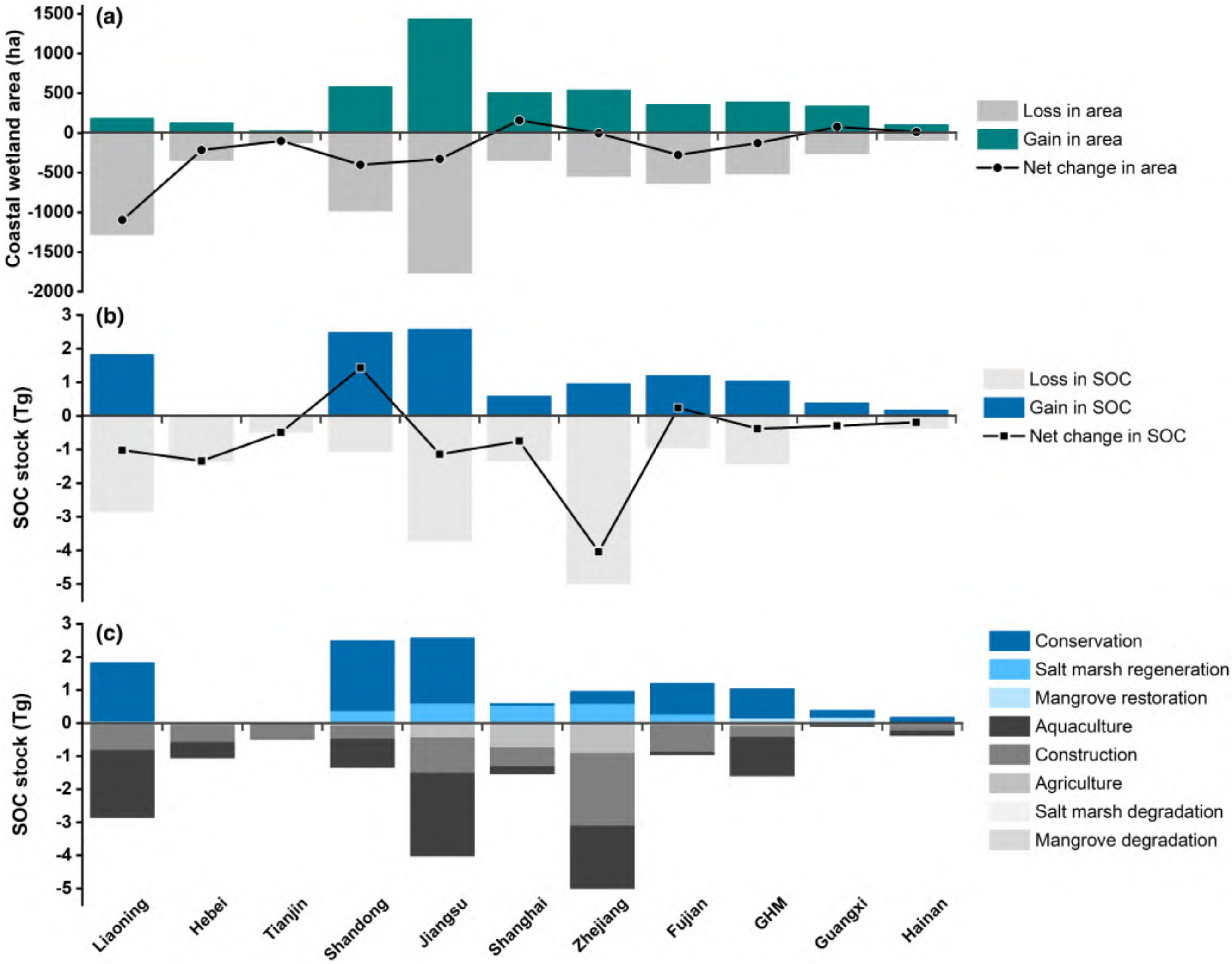

FIGURE 4 The loss and gain of coastal wetland area and SOC stock across coastal provinces over the last 30 years. Coastal wetland area (a). SOC stock (b). Natural and anthropogenic drivers on the loss and gain of SOC stock (c). GHM is the Guangdong-Hong Kong-Macao area.

already exists (Sanderman et al., 2018), the base year for this map is 2000 and does not cover many mangrove areas in China as the area of mangroves in China has increased since 2000. Currently, no map of SOC stocks has been developed for China's salt marshes, seagrass beds, and mudflats. In our study, we extracted the spatial distribution of three coastal wetlands with high accuracy (more than 90%) and used 262 SOC sampling sites in mangroves, salt marshes, and mudflats to produce their SOC stock maps based on the BRT model. Our developed map of SOC stocks can identify the hot spots and cold spots of carbon-rich areas in China's coastal wetlands, which are invaluable for the improvement of blue carbon management and sustainability in China. Seagrass bed was not included in our study because the spatial distribution of seagrass beds in China is uncertain and few sampling sites in published studies are available.

Our results suggested that the SOC stocks in China's coastal wetlands were 77.8 Tg C with 3.6 Tg C in mangroves, 8.8 Tg C in salt marshes, and 65.4 Tg C in mudflats (Table 1). SOC stocks of mangroves in the previous study were 6.3 Tg C (Fu et al., 2021) and were overestimated due to simpler algorithms. SOC stocks of mudflats in the previous study were 78.07 Tg C (Chen et al., 2020) and were overestimated due to the use of overestimated mudflat area (Murray et al., 2019). Many aquaculture ponds in China's coastal areas were misclassified as mudflats in Murray's study because the bottom soil of aquaculture ponds is exposed during the dry season (Pekel et al., 2016). The SOC density in mangroves and salt marshes were 166.9 ± 47.7 Mg C/ha and 86.8 ± 67.8 Mg C/ha, respectively, which were lower than the results in previous studies (Liu et al., 2014; Meng et al., 2019) and the global mean value (Duarte et al., 2013). This may be due to the limited data used in early studies and field observation of SOC-rich areas, resulting in the overestimation of SOC stocks. China's coastal rivers account for nearly 12% of the global sediment delivered into the ocean (Milliman & Farnsworth, 2013), which resulted in the decline of particulate organic carbon in coastal rivers and explained why the SOC stock in China's mangroves and salt marshes was lower than the global mean value.

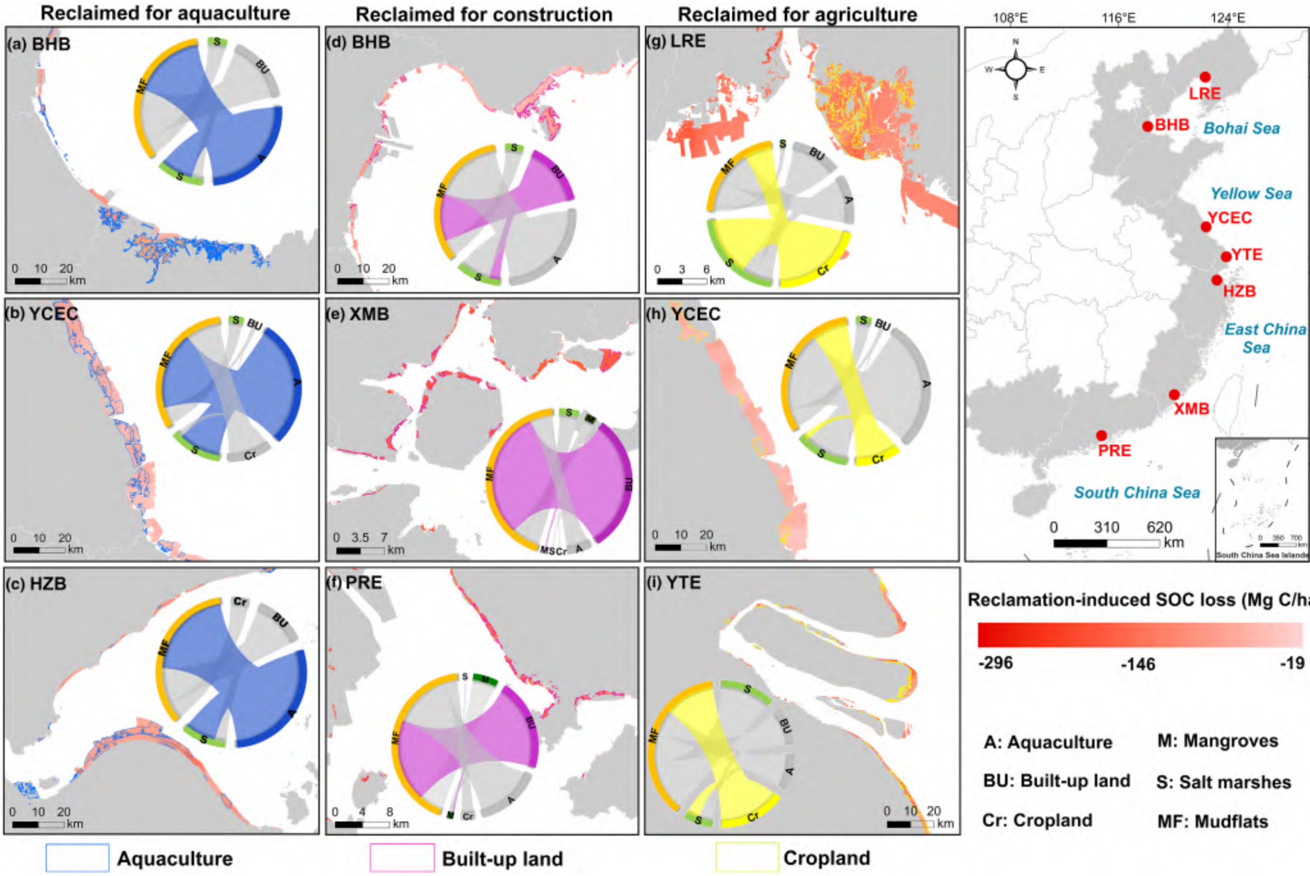

FIGURE 5 Spatial pattern of the reclamation-induced SOC loss in China's coastal wetlands and the amount of SOC loss caused by multiple reclamation activities in typical estuaries. Spatial pattern of the aquaculture-induced SOC loss in the Bohai Bay (BHB) (a), Yancheng Estuary Cluster (YCEC) (b), Hangzhou Bay (HZB) (c). Spatial pattern of SOC loss caused by construction activities in the Bohai Bay (d), Xiamen Bay (XMB) (e), and Pearl River Estuary (PRE) (f). Spatial pattern of SOC loss induced by agriculture activities in the Liao River Estuary (LRE) (g), Yancheng Estuary Cluster (h), and Yangtze Estuary (YTZ) (i). The colors in the Circos plots represent SOC flow from one coastal wetland to one land use, and the gray color represents the change in SOC driven by reclamation/landcover changes not currently being emphasized. The width of the lines represents the amount of SOC flow. Map lines delineate study areas and do not necessarily depict accepted national boundaries.

4.2 | Principal driving factors affecting the resilience of blue carbon stocks

Blue carbon stocks in China's coastal wetlands were controlled by climate factors and marine environmental factors (Figure 3). There were significant positive effects of the mean annual minimum SST on mangrove SOC stocks. Mangroves, extremely sensitive to the minimum SST, would face the threat of death and functional decline when the minimum SST was lower than a certain threshold (Cavanaugh et al., 2018). Inversely, the mangrove SOC stocks would be enhanced within a suitable SST (Lewis et al., 2020; Serrano et al., 2019). For example, the SOC stock in mangrove forests increased twice when the minimum SST was between 18 and 20°C in our study (Figure S5). Given that China's mangroves are located in the tropical and subtropical coasts, we believe that there is an optimal metabolic temperature for mangrove forests in carbon sequestration with a warming climate, and the SOC stock would decrease once the temperature is higher than the metabolic optimum of mangrove forests. This optimal metabolic temperature has been demonstrated in local tidal marsh and mangrove ecosystems based on field experiments in previous studies (Coldren et al., 2016; Smith et al., 2022).

There were significant positive effects of the mean annual precipitation on the SOC stocks across all coastal wetlands. Generally, greater rainfall is associated with longer soil inundation periods, and resulting in an increase in water-logged soils, which may contribute to a lower SOC decomposition rate and higher SOC burial (Sanders et al., 2016; Spivak et al., 2019). Salinity plays a key role in promoting SOC stocks in salt marshes. The increase of marine salinity results in the weakened metabolic capacity of soil microorganisms and slows down the SOC decomposition rate with the addition of a salt, which is conducive to SOC accumulation and storage (Chambers et al., 2013; Hinson et al., 2019). However, too much rainfall may also result in longer inundation of coastal wetlands on high-tide levels, which in turn causes increased salinity and the death of some salt-intolerant species (Crase et al., 2013), ultimately resulting in a decrease in SOC stocks. Therefore, optimal rainfall and salinity across different coastal wetlands that promote carbon sinks need to be identified in the future.

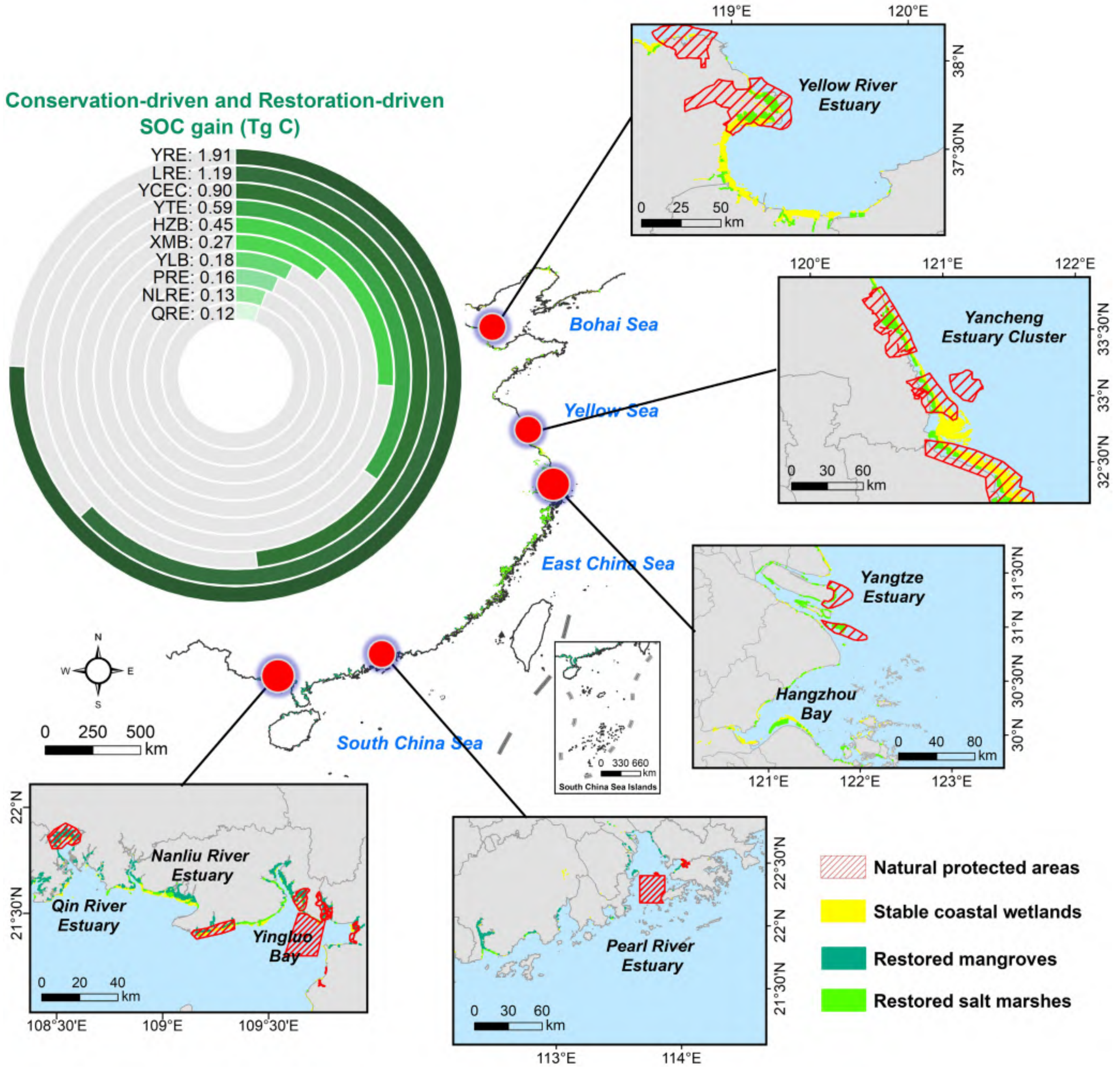

FIGURE 6 The spatial distribution of conserved and restored coastal wetlands and the number of SOC gains driven by conservation and restoration. Map lines delineate study areas and do not necessarily depict accepted national boundaries.

TSM (an agent of sediment supply) has no significant effect on the SOC stocks of coastal wetlands in our study, but reduced sediment supplies due to human activities will affect the ability of coastal wetlands to accumulate carbon, especially if the rate of sea-level rise exceeds the sedimentation rate (Saintilan et al., 2020). As CO_2 levels are rising and the globe is warming, the blue carbon stock in coastal wetlands is facing severe climate and marine risks in the future. Some empirical studies demonstrate that elevated CO_2 concentration can increase vertical accretion and elevation gain, and then enhance the carbon sinks in coastal wetlands (Langley et al., 2009; Reef et al., 2017). However, recent evidence revealed accelerated sea-level rise is suppressing CO_2 stimulation of tidal marsh productivity (Zhu et al., 2022). Therefore, the interaction of elevated CO_2, decreased sediment supplies, and rising sea levels need to be addressed to enhance the resilience of coastal wetlands to future climate and marine risks.

4.3 | Implications for coastal wetlands management and resilience enhancement

Coastal wetlands in China have lost over 24,000 ha/year during the past decades, reclaimed for agriculture and salt pans from 1950 to 1970, aquaculture, and built-up areas from 1980 to 2015 (Wang

TABLE 3 Net change in area and SOC stock of China's coastal wetlands during 1990–2020.

Provinces	Net change in area (km^2)	Net change in SOC stock (Tg C)
Liaoning	−1098.6	−1.0
Hebei	−216.2	−1.0
Tianjin	−100.4	−0.5
Shandong	−400.6	1.1
Jiangsu	−328.9	−1.4
Shanghai	159.3	−1.0
Zhejiang	−4.5	−4.0
Fujian	−277.4	0.2
GHM (Guangdong-Hong Kong-Macao area)	−127.8	−0.6
Guangxi	75.4	0.3
Hainan	13.0	−0.2
Total	−2306.7	−8.1

Note: Negative values are the net loss in area/SOC stock. Positive values are the net gain in area/SOC stock.

et al., 2014). Our results suggested aquaculture drove the most SOC loss in China's coastal provinces, which accounted for 50% of the total SOC loss during the past 30 years (Table S4). Nutrient import from aquaculture ponds leads to further wetland losses and promotes the decomposition of buried SOC (Atwood et al., 2017; Deegan et al., 2012). China has the largest aquaculture industry worldwide, mainly concentrated in Bohai Bay, Jiangsu, and Guangdong, where coastal wetlands are also rich (Duan et al., 2020), which induced more eutrophication (Xiao et al., 2019) and suggested further loss risk of SOC stocks in these regions. Additionally, we found that Shanghai, Zheijang, and Guangxi presented a net increase in wetland area but a net decrease in SOC stock during the past 30 years. The reason behind this contradiction is that a lot of mudflats with high SOC density were reclaimed for land use (e.g., aquaculture, construction, and agriculture) in these provinces. Although decreased mudflats can be offset by wetland restoration, increased SOC stock is much lower than decreased SOC stock. Therefore, there is a need for more actions to restore and protect coastal wetlands (especially mudflats, which account for 86.1% of total SOC stocks in China's coastal wetlands) from the loss of reclamation and induced eutrophication in these regions.

Over the past decades, China has made great efforts in coastal wetland conservation and restoration, as signified by the implementation of multiple coastal wetland conservation and restoration projects (National Development and Reform Commission of China, 2016), the construction of coastal wetland nature reserves, the practice of ecological civilization, special action plan for mangrove protection and restoration (2020–2025; National Forestry and Grassland Administration, 2020), etc. These national programs provided a major driver for coastal wetland area restoration (Wang et al., 2021). Furthermore, our findings proved that China's conservation and restoration actions effectively recovered lost blue carbon stocks in coastal wetlands. In our study, the estimated SOC gains driven by conservation and restoration in China's coastal wetlands were 11.3 Tg C during the last 30 years and can offset the reclamation-induced SOC losses by 58.2%, which indicated great achievements in the conservation and restoration of China's coastal wetlands over the last 30 years (Figure S6). The estimated SOC gains following conservation and restoration over the last 30 years in our study had also some uncertainty since the CAR data collected from published literature represented the mean value of CAR over the past 20–100 years.

Increasing coastal wetland areas is the first step to enhancing blue carbon sinks in current conservation strategy of China's coastal wetlands. Enhancing the carbon sequestration capacity of existing coastal wetlands needs further consideration in coastal wetland management, as our study found that 75.4% of SOC stocks were gained from unchanged coastal wetlands over the last three decades. However, the SOC stock in existing coastal wetlands would be exposed to threats of land-sea warming (Fan & Li, 2022), *Spartina alterniflora* invasion (Xia et al., 2021), and sea-level rise (Wang et al., 2019). The SOC stocks in mangroves and salt marshes might be substantially reduced after *S. alterniflora* invasion (Xu et al., 2022), and more efforts are suggested to focus on restoring native vegetation. For the mangrove ecosystem, forest thinning with mixed species along the seaward fringe was an effective nature-based solution for preventing *S. alterniflora* invasion and enhancing the organic carbon sink (Chen et al., 2021). Although carbon accumulation capacity in some coastal wetlands might be enhanced with accelerating sea level rise due to more sediment supply (Herbert et al., 2021), a large SOC stock of coastal wetlands might be lost owing to changed hydrology and increased salinity. Therefore, optimizing tree species structure, restoring sediment availability, and improving hydrological connectivity are needed to mitigate climatic risks and enhance the resilience of blue carbon ecosystems in the future.

5 | CONCLUSIONS

Coastal wetlands are important in CO_2 sequestration but are sensitive to climate changes and anthropogenic disturbances. Our study explores the spatial pattern, driving factors, and loss and gain of SOC stocks in China's coastal wetlands over three decades. SOC stocks in China's coastal wetlands were 77.8 Tg C with 3.6 Tg C in mangroves, 8.8 Tg C in salt marshes, and 65.4 Tg C in mudflats. The high-resolution SOC map can identify the hot spots (Hainan and Guangxi) and cold spots (Shandong and Jiangsu) of carbon-rich areas in China's coastal wetlands, which are invaluable for the improvement of blue carbon management and sustainability in China. Estimated blue carbon gains driven by conservation and restoration in China's coastal wetlands were 11.3 Tg C during the last 30 years, which can offset the reclamation-induced losses by 58.2% during this period. It proved that China's conservation and restoration actions had significant effects on effectively recovering the blue carbon stocks. Identifying optimal metabolic temperature and salinity, restoring sediment availability, and improving hydrological connectivity are priorities for enhancing coastal wetland resilience to anthropogenic and climatic risks in the future.

AUTHOR CONTRIBUTIONS

Bingxiong Fan: Conceptualization; formal analysis; funding acquisition; investigation; methodology; visualization; writing – original draft; writing – review and editing. **Yangfan Li:** Conceptualization; funding acquisition; investigation; resources; supervision; writing – review and editing.

ACKNOWLEDGMENTS

This work was funded by the National Natural Science Foundation of China Grants (no. 42276232), the China Postdoctoral Science Foundation (no. 2023M732933), and the Internal Program of State Key Laboratory of Marine Environmental Science (no. MELRI2205). We appreciate Dr. Yi Li and Mr. Zheng Li at Xiamen University, who provided valuable comments and suggestions for this study. We also thank Dr. Zhen Zhang for the data provision and valuable comments.

CONFLICT OF INTEREST STATEMENT

The authors reported no potential conflict of interest.

DATA AVAILABILITY STATEMENT

The data that support the findings of this study are openly available in Figshare at https://doi.org/10.6084/m9.figshare.24483622.

ORCID

Yangfan Li https://orcid.org/0000-0002-5419-7051

REFERENCES

Armitage, A. R., & Fourqurean, J. W. (2016). Carbon storage in seagrass soils: Long-term nutrient history exceeds the effects of near-term nutrient enrichment. *Biogeosciences*, *13*(1), 313–321. https://doi.org/10.5194/bg-13-313-2016

Atwood, T. B., Connolly, R. M., Almahasheer, H., Carnell, P. E., Duarte, C. M., Ewers Lewis, C. J., & Lovelock, C. E. (2017). Global patterns in mangrove soil carbon stocks and losses. *Nature Climate Change*, *7*(7), 523–528. https://doi.org/10.1038/nclimate3326

Bargiel, D. (2017). A new method for crop classification combining time series of radar images and crop phenology information. *Remote Sensing of Environment*, *198*, 369–383. https://doi.org/10.1016/j.rse.2017.06.022

Carnell, P. E., Windecker, S. M., Brenker, M., Baldock, J., Masque, P., Brunt, K., & Macreadie, P. I. (2018). Carbon stocks, sequestration, and emissions of wetlands in south eastern Australia. *Global Change Biology*, *24*(9), 4173–4184. https://doi.org/10.1111/gcb.14319

Cavanaugh, K. C., Osland, M. J., Bardou, R., Hinojosa-Arango, G., López-Vivas, J. M., Parker, J. D., & Rovai, A. S. (2018). Sensitivity of mangrove range limits to climate variability. *Global Ecology and Biogeography*, *27*(8), 925–935. https://doi.org/10.1111/geb.12751

Chambers, L. G., Osborne, T. Z., & Reddy, K. R. (2013). Effect of salinity-altering pulsing events on soil organic carbon loss along an intertidal wetland gradient: A laboratory experiment. *Biogeochemistry*, *115*(1–3), 363–383. https://doi.org/10.1007/s10533-013-9841-5

Chen, J., Cao, X., Peng, S., & Ren, H. (2017). Analysis and applications of GlobeLand30: A review. *ISPRS International Journal of Geo-Information*, *6*(8), 230–238. https://doi.org/10.3390/ijgi6080230

Chen, J., Wang, D., Li, Y., Yu, Z., Chen, S., Hou, X., White, J. R., & Chen, Z. (2020). The carbon stock and sequestration rate in tidal flats from coastal China. *Global Biogeochemical Cycles*, *34*(11), e2020GB006772. https://doi.org/10.1029/2020GB006772

Chen, L., Lin, Q., Krauss, K. W., Zhang, Y., Cormier, N., & Yang, Q. (2021). Forest thinning in the seaward fringe speeds up surface elevation increment and carbon accumulation in managed mangrove forests. *Journal of Applied Ecology*, *58*(9), 1899–1909. https://doi.org/10.1111/1365-2664.13939

Coldren, G. A., Barreto, C. R., Wykoff, D. D., Morrissey, E. M., Langley, J. A., Feller, I. C., & Chapman, S. K. (2016). Chronic warming stimulates growth of marsh grasses more than mangroves in a coastal wetland ecotone. *Ecology*, *97*(11), 3167–3175. https://doi.org/10.1002/ecy.1539

Crase, B., Liedloff, A., Vesk, P. A., Burgman, M. A., & Wintle, B. A. (2013). Hydroperiod is the main driver of the spatial pattern of dominance in mangrove communities. *Global Ecology and Biogeography*, *22*(7), 806–817. https://doi.org/10.1111/geb.12063

Davidson, N. C. (2014). How much wetland has the world lost? Long-term and recent trends in global wetland area. *Marine and Freshwater Research*, *65*(10), 934. https://doi.org/10.1071/MF14173

Duarte de Paula Costa, M., Lovelock, C. E., Waltham, N. J., Young, M., Adame, M. F., Bryant, C. V., Butler, D., Green, D., Rasheed, M. A., Salinas, C., Serrano, O., York, P. H., Whitt, A. A., & Macreadie, P. I. (2021). Current and future carbon stocks in coastal wetlands within the Great Barrier Reef catchments. *Global Change Biology*, *27*(14), 3257–3271. https://doi.org/10.1111/gcb.15642

Deegan, L. A., Johnson, D. S., Warren, R. S., Peterson, B. J., Fleeger, J. W., Fagherazzi, S., & Wollheim, W. M. (2012). Coastal eutrophication as a driver of salt marsh loss. *Nature*, *490*(7420), 388–392. https://doi.org/10.1038/nature11533

DeGryze, S., Six, J., Paustian, K., Morris, S. J., Paul, E. A., & Merckx, R. (2004). Soil organic carbon pool changes following land-use conversions. *Global Change Biology*, *10*(7), 1120–1132. https://doi.org/10.1111/j.1529-8817.2003.00786.x

Donato, D. C., Kauffman, J. B., Murdiyarso, D., Kurnianto, S., Stidham, M., & Kanninen, M. (2011). Mangroves among the most carbon-rich forests in the tropics. *Nature Geoscience*, *4*(5), 293–297. https://doi.org/10.1038/ngeo1123

Duan, Y., Li, X., Zhang, L., Chen, D., & Ji, H. (2020). Mapping national-scale aquaculture ponds based on the Google earth engine in the Chinese coastal zone. *Aquaculture*, *520*, 734666. https://doi.org/10.1016/j.aquaculture.2019.734666

Duarte, C. M., Losada, I. J., Hendriks, I. E., Mazarrasa, I., & Marbà, N. (2013). The role of coastal plant communities for climate change mitigation and adaptation. *Nature Climate Change*, *3*(11), 961–968. https://doi.org/10.1038/nclimate1970

Elith, J., Leathwick, J. R., & Hastie, T. (2008). A working guide to boosted regression trees. *The Journal of Animal Ecology*, *77*(4), 802–813. https://doi.org/10.1111/j.1365-2656.2008.01390.x

Fan, B. X., & Li, Y. F. (2022). Coupled land-sea warming dominates the net land carbon uptake variability in the Greater Bay Area of South China. *Earth's Futures*, *10*(8), e2021EF002556. https://doi.org/10.1029/2021EF002556

Fan, B. X., Li, Y. F., & Pavao-Zuckerman, M. (2021). The dynamics of land-sea-scape carbon flow can reveal anthropogenic destruction and restoration of coastal carbon sequestration. *Landscape Ecology*, *36*, 1933–1949. https://doi.org/10.1007/s10980-020-01148-9

Fu, C., Li, Y., Zeng, L., Zhang, H., Tu, C., Zhou, Q., Xiong, K., Wu, J., Duarte, C. M., Christie, P., & Luo, Y. (2021). Stocks and losses of soil organic carbon from Chinese vegetated coastal habitats. *Global Change Biology*, *27*(1), 202–214. https://doi.org/10.1111/gcb.15348

Galatowitsch, S. M. (2018). Natural and anthropogenic drivers of wetland change. In *The wetland book II: Distribution, description, and conservation*. Springer Nature Press.

Hagger, V., Worthington, T. A., Lovelock, C. E., Adame, M. F., Amano, T., Brown, B. M., & Saunders, M. I. (2022). Drivers of global mangrove loss and gain in social-ecological systems. *Nature Communications*, *13*(1), 6373. https://doi.org/10.1038/s41467-022-33962-x

Herbert, E. R., Windham-Myers, L., & Kirwan, M. L. (2021). Sea-level rise enhances carbon accumulation in United States tidal wetlands. *One Earth*, *4*(3), 425–433. https://doi.org/10.1016/j.oneear.2021.02.011

Hinson, A. L., Feagin, R. A., & Eriksson, M. (2019). Environmental controls on the distribution of tidal wetland soil organic carbon in the continental United States. *Global Biogeochemical Cycles*, *33*(11), 1408–1422. https://doi.org/10.1029/2019GB006179

Holmquist, J. R., Brown, L. N., & MacDonald, G. M. (2021). Localized scenarios and latitudinal patterns of vertical and lateral resilience of tidal marshes to sea-level rise in the contiguous United States. *Earth's Futures*, *9*(6), e2020EF001804. https://doi.org/10.1029/2020EF001804

Hu, L., Li, W., & Xu, B. (2018). Monitoring mangrove forest change in China from 1990 to 2015 using Landsat-derived spectral-temporal variability metrics. *International Journal of Applied Earth Observation and Geoinformation*, *73*, 88–98. https://doi.org/10.1016/j.jag.2018.04.001

Huang, Y., Ciais, P., Santoro, M., Makowski, D., Chave, J., Schepaschenko, D., Abramoff, R. Z., Goll, D. S., Yang, H., Chen, Y., Wei, W., & Piao, S. L. (2021). A global map of root biomass across the world's forests. *Earth System Science Data*, *13*, 4263–4274. https://doi.org/10.5194/essd-13-4263-2021

Jouffray, J. B., Wedding, L. M., Norström, A. V., Donovan, M. K., Williams, G. J., Crowder, L. B., Erickson, A. L., Friedlander, A. M., Graham, N. A. J., Gove, J. M., Kappel, C. V., Kittinger, J. N., Lecky, J., Oleson, K. L. L., Selkoe, K. A., White, C., Williams, I. D., & Nyström, M. (2019). Parsing human and biophysical drivers of coral reef regimes. *Proceedings of the Royal Society B: Biological Sciences*, *286*(1896), 20182544. https://doi.org/10.1098/rspb.2018.2544

Langley, J. A., McKee, K. L., Cahoon, D. R., Cherry, J. A., & Megonigal, J. P. (2009). Elevated CO_2 stimulates marsh elevation gain, counterbalancing sea-level rise. *Proceedings of the National Academy of Sciences of the United States of America*, *106*(15), 6182–6186. https://doi.org/10.1073/pnas.0807695106

Lewis, C., Young, M. A., Ierodiaconou, D., Baldock, J. A., & Macreadie, P. I. (2020). Drivers and modelling of blue carbon stock variability. *Biogeosciences*, *17*, 2041–2059. https://doi.org/10.5194/bg-17-2041-2020

Li, Z., Zan, Q., Yang, Q., Zhu, D., Chen, Y., & Yu, S. (2019). Remote estimation of mangrove aboveground carbon stock at the species level using a low-cost unmanned aerial vehicle system. *Remote Sensing*, *11*(9), 1018. https://doi.org/10.3390/rs11091018

Liu, H., Ren, H., Hui, D., Wang, W., Liao, B., & Cao, Q. (2014). Carbon stocks and potential carbon storage in the mangrove forests of China. *Journal of Environmental Management*, *133*, 86–93. https://doi.org/10.1016/j.jenvman.2013.11.037

Lovelock, C. E., & Reef, R. (2020). Variable impacts of climate change on blue carbon. *One Earth*, *3*(2), 195–211. https://doi.org/10.1016/j.oneear.2020.07.010

Ma, Z. J., Melville, D. S., Liu, J. G., Chen, Y., Yang, H. Y., Ren, W. W., Zhang, Z. W., Piersma, T., & Li, B. (2014). Rethinking China's new great wall. *Science*, *346*(6212), 912–914. https://doi.org/10.1126/science.1257258

Macreadie, P. I., Costa, M. D., Atwood, T. B., Friess, D. A., Kelleway, J. J., Kennedy, H., Lovelock, C. E., Serrano, O., & Duarte, C. M. (2021). Blue carbon as a natural climate solution. *Nature Reviews Earth and Environment*, *2*(12), 826–839. https://doi.org/10.1038/s43017-021-00224-1

Mcleod, E., Chmura, G. L., Bouillon, S., Salm, R., Björk, M., Duarte, C. M., Lovelock, C. E., Schlesinger, W. H., & Silliman, B. R. (2011). A blueprint for blue carbon: Toward an improved understanding of the role of vegetated coastal habitats in sequestering CO_2. *Frontiers in Ecology and the Environment*, *9*(10), 552–560. https://doi.org/10.1890/110004

Meng, W., Feagin, R. A., Hu, B., He, M., & Li, H. (2019). The spatial distribution of blue carbon in the coastal wetlands of China. *Estuarine, Coastal and Shelf Science*, *222*, 13–20. https://doi.org/10.1016/j.ecss.2019.03.010

Milliman, J. D., & Farnsworth, K. L. (2013). *River discharge to the coastal ocean: A global synthesis*. Cambridge University Press.

Murray, N. J., Phinn, S. R., DeWitt, M., Ferrari, R., Johnston, R., Lyons, M. B., Clinton, N., Thau, D., & Fuller, R. A. (2019). The global distribution and trajectory of tidal flats. *Nature*, *565*(7738), 222–225. https://doi.org/10.1038/s41586-018-0805-8

National Development and Reform Commission of China. (2016). The 13th five-year plan for economic and social development of the People's Republic of China. Retrieved from https://www.gov.cn/xinwen/2016-03/17/content_5054992.htm?url_type=39&object_type=webpage&pos=1

National Forestry and Grassland Administration. (2020). Special action plan for mangrove protection and restoration in the People's Republic of China. Retrieved from http://www.forestry.gov.cn/main/3957/20200828/145505777366697.html

Nellemann, C., Corcoran, E., Duarte, C. M., Luis, V., Cassandra, D. Y., Luciano, F., & Gabriel, G. (2009). Blue carbon: The role of healthy oceans in binding carbon. A rapid response assessment. United Nations Environment Programme, GRID-Arendal.

Ouyang, X., & Lee, S. Y. (2020). Improved estimates on global carbon stock and carbon pools in tidal wetlands. *Nature Communications*, *11*(1), 317. https://doi.org/10.1038/s41467-019-14120-2

Pekel, J. F., Cottam, A., Gorelick, N., & Belward, A. S. (2016). High-resolution mapping of global surface water and its long-term changes. *Nature*, *540*(7633), 418–422. https://doi.org/10.1038/nature20584

Pendleton, L., Donato, D. C., Murray, B. C., Crooks, S., Jenkins, W. A., Sifleet, S., Craft, C., Fourqurean, J. W., Kauffman, J. B., Marbà, N., Megonigal, P., Pidgeon, E., Herr, D., Gordon, D., & Baldera, A. (2012). Estimating global "blue carbon" emissions from conversion and degradation of vegetated coastal ecosystems. *PLoS One*, *7*(9), e43542. https://doi.org/10.1371/journal.pone.0043542

Reef, R., Spencer, T., Möller, I., Lovelock, C. E., Christie, E. K., McIvor, A. L., & Tempest, J. A. (2017). The effects of elevated CO_2 and eutrophication on surface elevation gain in a European salt marsh. *Global Change Biology*, *23*(2), 881–890. https://doi.org/10.1111/gcb.13396

Rogers, K., Kelleway, J. J., Saintilan, N., Megonigal, J. P., Adams, J. B., & Holmquist, J. R. (2019a). Wetland carbon storage controlled by millennial-scale variation in relative sea-level rise. *Nature*, *567*, 91–95. https://doi.org/10.1038/s41586-019-0951-7

Rogers, K., Saintilan, N., Mazumder, D., & Kelleway, J. J. (2019b). Mangrove dynamics and blue carbon sequestration. *Biology Letters*, *15*(3), 20180471. https://doi.org/10.1098/rsbl.2018.0471

Saintilan, N., Khan, N. S., Ashe, E., Kelleway, J. J., Rogers, K., Woodroffe, C. D., & Horton, B. P. (2020). Thresholds of mangrove survival under rapid sea level rise. *Science*, *368*(6495), 1118–1121. https://doi.org/10.1126/science.aba26

Sajjad, M., Li, Y., Tang, Z., Cao, L., & Liu, X. (2018). Assessing hazard vulnerability, habitat conservation, and restoration for the enhancement of mainland China's coastal resilience. *Earth's Future*, *6*(3), 326–338. https://doi.org/10.1002/2017EF000676

Salinas, C., Duarte, C. M., Lavery, P. S., Masque, P., Arias-Ortiz, A., Leon, J. X., Callaghan, D., Kendrick, G. A., & Serrano, O. (2020). Seagrass losses since mid-20th century fuelled CO_2 emissions from soil carbon stocks. *Global Change Biology*, *26*(9), 4772–4784. https://doi.org/10.1111/gcb.15204

Sanderman, J., Hengl, T., Fiske, G., Solvik, K., Adame, M. F., Benson, L., Bukoski, J. J., Carnell, P., Cifuentes-Jara, M., Donato, D., Duncan, C., Eid, E. M., Ermgassen, P., Lewis, C. J. E., Macreadie, P. I., Glass, L., Gress, S., Jardine, S. L., Jones, T. G., … Landis, E. (2018). A global map of mangrove forest soil carbon at 30 m spatial resolution. *Environmental Research Letters*, *13*(5), 55002. https://doi.org/10.1088/1748-9326/aabe1c

Sanders, C. J., Maher, D. T., Tait, D. R., Williams, D., Holloway, C., & Sippo, J. Z. (2016). Are global mangrove carbon stocks driven by rainfall? *Journal of Geophysical Research: Biogeosciences*, *121*, 2600–2609. https://doi.org/10.1002/2016JG003510

Serrano, O., Lovelock, C. E., Atwood, B. T., Macreadie, P. I., Canto, R., & Phinn, S. (2019). Australian vegetated coastal ecosystems as global hotspots for climate change mitigation. *Nature Communications*, *10*, 4313. https://doi.org/10.1038/s41467-019-12176-8

Simard, M., Fatoyinbo, L., Smetanka, C., Rivera-Monroy, V. H., Castañeda-Moya, E., Thomas, N., & Van der Stocken, T. (2019). Mangrove canopy height globally related to precipitation, temperature and cyclone frequency. *Nature Geoscience*, *12*(1), 40–45. https://doi.org/10.1038/s41561-018-0279-1

Smith, A. J., Noyce, G. L., Megonigal, J. P., Guntenspergen, G. R., & Kirwan, M. L. (2022). Temperature optimum for marsh resilience and carbon accumulation revealed in a whole-ecosystem warming experiment. *Global Change Biology*, *28*(10), 3236–3245. https://doi.org/10.1111/gcb.16149

Spawn, S. A., Sullivan, C. C., Lark, T. J., & Gibbs, H. K. (2020). Harmonized global maps of above and belowground biomass carbon density in the year 2010. *Scientific Data*, *7*, 112. https://doi.org/10.1038/s41597-020-0444-4

Spivak, A. C., Sanderman, J., Bowen, J. L., Canuel, E. A., & Hopkinson, C. S. (2019). Global-change controls on soil-carbon accumulation and loss in coastal vegetated ecosystems. *Nature Geoscience*, *12*, 685–692. https://doi.org/10.1038/s41561-019-0435-2

Wang, F., Lu, X., Sanders, C. J., & Tang, J. (2019). Tidal wetland resilience to sea level rise increases their carbon sequestration capacity in United States. *Nature Communications*, *10*(1), 5434. https://doi.org/10.1038/s41467-019-13294-z

Wang, W., Liu, H., Li, Y., & Su, J. (2014). Development and management of land reclamation in China. *Ocean & Coastal Management*, *102*, 415–425. https://doi.org/10.1016/j.ocecoaman.2014.03.009

Wang, X., Xiao, X., Xu, X., Zou, Z., Chen, B., Qin, Y., Zhang, X., Dong, J., Liu, D., Pan, L., & Li, B. (2021). Rebound in China's coastal wetlands following conservation and restoration. *Nature Sustainability*, *4*(12), 1076–1083. https://doi.org/10.1038/s41893-021-00793-5

Wang, X., Xiao, X., Zou, Z., Hou, L., Qin, Y., Dong, J., & Li, B. (2020). Mapping coastal wetlands of China using time series Landsat images in 2018 and Google Earth Engine. *ISPRS Journal of Photogrammetry and Remote Sensing*, *163*, 312–326. https://doi.org/10.1016/j.isprsjprs.2020.03.014

Xia, S., Wang, W., Song, Z., Kuzyakov, Y., Guo, L., Van Zwieten, L., & Wang, H. (2021). *Spartina alterniflora* invasion controls organic carbon stocks in coastal marsh and mangrove soils across tropics and subtropics. *Global Change Biology*, *27*(8), 1627–1644. https://doi.org/10.1111/gcb.15516

Xiao, X., Agustí, S., Pan, Y., Yu, Y., Li, K., Wu, J., & Duarte, C. M. (2019). Warming amplifies the frequency of harmful algal blooms with eutrophication in Chinese coastal waters. *Environmental Science & Technology*, *53*(22), 13031–13041. https://doi.org/10.1021/acs.est.9b03726

Xu, X., Wei, S., Chen, H., Li, B., & Nie, M. (2022). Effects of Spartina invasion on the soil organic carbon content in salt marsh and mangrove ecosystems in China. *Journal of Applied Ecology*, *59*(7), 1937–1946. https://doi.org/10.1111/1365-2664.14202

Zhang, Z., Xu, N., Li, Y. F., & Li, Y. (2022). Sub-continental-scale mapping of tidal wetland composition for East Asia: A novel algorithm integrating satellite tide-level and phenological features. *Remote Sensing of Environment*, *269*, 112799. https://doi.org/10.1016/j.rse.2021.112799

Zhu, C., Langley, J. A., Ziska, L. H., Cahoon, D. R., & Megonigal, J. P. (2022). Accelerated sea-level rise is suppressing CO_2 stimulation of tidal marsh productivity: A 33-year study. *Science Advances*, *8*(20), eabn0054. https://doi.org/10.1126/sciadv.abn0054

Zhu, Y., Liu, K., Liu, L., Wang, S., & Liu, H. (2015). Retrieval of mangrove aboveground biomass at the individual species level with worldview-2 images. *Remote Sensing*, *7*(9), 12192–12214. https://doi.org/10.3390/rs70912192

DATA SOURCES

Alongi, D. M., Pfitzner, J., Trott, L. A., Tirendi, F., Dixon, P., & Klumpp, D. (2005). Rapid sediment accumulation and microbial mineralization in forests of the mangrove *Kandelia Candel* in the Jiulongjiang Estuary, China. *Estuarine, Coastal and Shelf Science*, *63*, 605–618.

Bai, J., Zhang, G., Zhao, Q., Lu, Q., Jia, J., Cui, B., & Liu, X. (2016). Depth-distribution patterns and control of soil organic carbon in coastal salt marshes with different plant covers. *Scientific Reports*, *6*, 34835.

Bao, H., Wu, Y., Unger, D., Du, J., Herbeck, L. S., & Zhang, J. (2013). Impact of the conversion of mangroves into aquaculture ponds on the sedimentary organic matter composition in a tidal flat estuary (Hainan Island, China). *Continental Shelf Research*, *57*, 82–91.

Bao, K., Shen, J., Quan, G., & Liu, F. (2016). A 150-year isotopic record of lead deposition in Yancheng coastal wetland, China. *Chinese Geographical Science*, *26*, 755–769.

Bu, N., Qu, J., Li, G., Zhao, B., Zhang, R., & Fang, C. (2015). Reclamation of coastal salt marshes promoted carbon loss from previously-sequestered soil carbon pool. *Ecological Engineering*, *81*, 335–339.

Cao, L., Song, J., Li, X., Yuan, H., Li, N., Duan, L., & Wang, Q. (2015). Geochemical characteristics of soil C, N, P, and their stoichiometrical significance in the coastal wetlands of Laizhou Bay, Bohai Sea. *Clean-Soil Air Water*, *43*, 260–270.

Chen, G., Gao, M., Pang, B., Chen, S., & Ye, Y. (2018). Top-meter soil organic carbon stocks and sources in restored mangrove forests of different ages. *Forest Ecology and Management*, *422*, 87–94.

Chen, G., Tam, N. F. Y., & Ye, Y. (2010). Summer fluxes of atmospheric greenhouse gases N_2O, CH_4 and CO_2 from mangrove soil in South China. *Science of the Total Environment*, *408*, 2761–2767.

Chen, J., Wang, D., Li, Y., Yu, Z., Chen, S., Hou, X., White, J. R., & Chen, Z. (2020). The carbon stock and sequestration rate in tidal flats from coastal China. *Global Biogeochemical Cycles*, *34*(11), e2020GB006772.

Chen, L., Lin, Q., Krauss, K. W., Zhang, Y., Cormier, N., & Yang, Q. (2021). Forest thinning in the seaward fringe speeds up surface elevation increment and carbon accumulation in managed mangrove forests. *Journal of Applied Ecology*, *58*(9), 1899–1909.

Chen, S., Chen, B., Chen, G., Ji, J., & Chen, G. (2021). Higher soil organic carbon sequestration potential at a rehabilitated mangrove comprised of *Aegiceras corniculatum* compared to *Kandelia obovata*. *Science of the Total Environment*, *752*, 142279.

Ding, H., Yao, S., & Chen, J. (2014). Authigenic pyrite formation and re-oxidation as an indicator of an unsteady-state redox sedimentary environment: Evidence from the intertidal mangrove sediments of Hainan Island, China. *Continental Shelf Research*, *78*, 85–99.

Feng, J., Cui, X., Zhou, J., Wang, L., Zhu, X., & Lin, G. (2019). Effects of exotic and native mangrove forests plantation on soil organic carbon, nitrogen, and phosphorus contents and pools in Leizhou, China. *Catena*, *180*, 1–7.

Feng, J., Zhou, J., Wang, L., Cui, X., Ning, C., Wu, H., & Lin, G. (2017). Effects of short-term invasion of *Spartina alterniflora* and the subsequent restoration of native mangroves on the soil organic carbon, nitrogen and phosphorus stock. *Chemosphere*, *184*, 774–783.

Fu, C., Li, Y., Zeng, L., Zhang, H., Tu, C., Zhou, Q., Xiong, K., Wu, J., Duarte, C. M., Christie, P., & Luo, Y. (2021). Stocks and losses of soil organic carbon from Chinese vegetated coastal habitats. *Global Change Biology*, *27*(1), 202–214.

Gan, H., Lin, J., Liang, K., & Xia, Z. (2013). Selected trace metals (As, Cd and Hg) distribution and contamination in the coastal wetland sediment of the northern Beibu Gulf, South China Sea. *Marine Pollution Bulletin*, *66*, 252–258.

Gao, J., Feng, Z., Chen, L., Wang, Y., Bai, F., & Li, J. (2016). The effect of biomass variations of *Spartina alterniflora* on the organic carbon content and composition of a salt marsh in northern Jiangsu Province, China. *Ecological Engineering*, *95*, 160–170.

Gao, T., Ding, D., Guan, W., & Liao, B. (2018). Carbon stocks of coastal wetland ecosystems on Hainan Island, China. *Polish Journal of Environmental Studies*, *27*(3), 1061–1069.

Gao, T., Guan, W., Mao, J., Jiang, Z., & Liao, B. (2017). Carbon storage and influence factors of major mangrove communities in Fucheng, Leizhou peninsula, Guangdong Province. *Ecology and Environmental Sciences*, *26*, 985–990. (in Chinese).

Gao, Y., Zhou, J., Wang, L., Guo, J., Feng, J., Wu, H., & Lin, G. (2019). Distribution patterns and controlling factors for the soil organic carbon in four mangrove forests of China. *Global Ecology and Conservation*, *17*, e00575.

Gao, Y. Q., Yuan, D. X., Lu, B. Y., Sun, L. M., Lin, H. Y., & Huang, S. Y. (2016). Spaciotemporal distribution of mercury in core sediments of the mangrove ecosystem in Jiulongjiang estuary. *Journal of Applied Oceanography*, *35*(1), 58–64. (in Chinese).

He, T., Sun, Z., Hu, X., Chen, B., Wang, H., & Wang, J. (2020). Effects of *Spartina alterniflora* invasion on spatial and temporal variations of total sulfur and inorganic sulfur fractions in sediments of salt marsh in the Min River estuary, Southeast China. *Ecological Indicators*, *113*, 106253.

He, Z., Sun, H., Yu, X., Yin, Z., Wu, M., Zhao, L., Hu, Z., Peng, Y., & Lee, S. Y. (2021). Monoculture or mixed culture? Relevance of fine root dynamics to carbon sequestration oriented mangrove afforestation and restoration. *Frontiers in Marine Science*, *8*, 763922.

Hou, D. L., He, D. J., Yan, J. Y., Wang, R., & Cai, J. B. (2016). Effect of invasive *Spartina alterniflora* on soil organic carbon in Eastern Fujian coastal wetlands. *Transactions of Oceanology and Limnology*, *1*, 68–76. (in Chinese).

Hou, X., Yin, P., Ding, X., Zhang, Y., & Bi, S. (2013). Carbon storage capacity in the Daguhe wetland, Jiaozhou Bay of Qingdao. *Marine Geology Frontiers*, *28*, 17–26. (in Chinese).

Hu, Y., Xu, Y., Xue, C., Luo, Y., Liao, B., & Zhu, N. (2019). Studies on carbon storages of *Sonneratia apetala* forest vegetation and soil in Guangdong Province. *Journal of South China Agricultural University*, *40*, 95–103. (in Chinese).

Hu, Y., Zhu, N., Liao, B., You, Y., & Tang, H. (2019). Carbon density and carbon fixation rate of mangroves of different restoration types in Qi'ao Island. *Journal of Central South University of Forestry & Technology*, *39*, 101–107. (in Chinese).

Huang, X., Wang, X., Li, X., Xin, K., Yan, Z., Sun, Y., & Bellerby, R. G. (2017). Distribution pattern and influencing factors for soil organic carbon (SOC) in mangrove communities at Dongzhaigang, China. *Journal of Coastal Research*, *34*, 434–442.

Jiang, Y. F., Du, J. Z., Zhang, J., Zhang, W. X., & Zhang, J. (2012). The determination of sedimentation rates in various vegetational zones of Chongming tidal flat of the Changjiang Estuary. *Acta Oceanologica Sinica*, *34*(2), 114–121. (in Chinese).

Jin, B., Lai, D. Y. F., Gao, D., Tong, C., & Zeng, C. (2017). Changes in soil organic carbon dynamics in a native C_4 plant-dominated tidal marsh following *Spartina alterniflora* invasion. *Pedosphere*, *27*, 856–867.

Kang, J., Meng, X. F., Xu, Y. Y., Luan, J., Long, X. H., & Liu, Z. P. (2012). Effects of different vegetation types on soil organic carbon pool in coastal saline-alkali soils of Jiangsu province. *The Soil*, *44*(2), 260–266. (in Chinese).

Li, C. X., Liu, Y. G., Liu, Z. X., Hu, Z. J., Bian, S. H., & Diao, S. B. (2008). Sediment transport and changes in scour and silting in the Quanzhou Bay. *Advances in Marine Science*, *1*, 26–34. (in Chinese).

Li, D., Xu, Y., Li, Y., Wang, J., Yin, X., Ye, X., & Wang, L. (2018). Sedimentary records of human activity and natural environmental evolution in sensitive ecosystems: A case study of a coral nature reserve in Dongshan Bay and a mangrove forest nature reserve in Zhangjiang River estuary, Southeast China. *Organic Geochemistry*, *121*, 22–35.

Li, M. (2018). *Carbon storage in the seagrass sediments of Guangxi China*. Nanning Normal University (in Chinese).

Li, R., Chai, M., Guo, M., & Qiu, G. Y. (2016). Sediment accumulation and mercury (Hg) flux in Avicennia marina forest of Deep Bay, China. *Estuarine, Coastal and Shelf Science*, *177*, 41–46.

Li, X. Y., Pu, L. J., Xu, Y., Xu, C. X., Zhu, M., Xu, C. Y., & Xie, X. F. (2020). Spatiotemporal heterogeneity of soil organic carbon in reclamation areas of tidal flat in North Jiangsu Province. *The Soil*, *52*(2), 365–371. (in Chinese).

Liao, C., Luo, Y., Jiang, L., Zhou, X., Wu, X., & Fang, C. (2007). Invasion of *Spartina alterniflora* enhanced ecosystem carbon and nitrogen stocks in the Yangtze estuary, China. *Ecosystems*, *10*, 1351–1361.

Liao, X. J., He, D. J., Wang, R., Cai, J. B., Su, S. C., & Zhang, Z. R. (2013). Distribution pattern of soil organic carbon contents in the coastal wetlands in eastern Fujian. *Wetland Science*, *11*(2), 192–197 (in Chinese).

Liu, J., Han, R., Su, H., Wu, Y., Zhang, L., Richardson, C. J., & Wang, G. (2017). Effects of exotic *Spartina alterniflora* on vertical soil organic carbon distribution and storage amount in coastal salt marshes in Jiangsu, China. *Ecological Engineering*, *106*, 132–139.

Liu, T., Liu, Y., & Le, Y. F. (2017). Response of mangrove swamp sedimentation rate to climate change. *Journal of Tropical Oceanography*, *36*(2), 40–47. (in Chinese).

Liu, Z., Pan, S., Liu, X., & Gao, J. (2010). Distribution of ^{137}Cs and ^{210}Pb in sediments of tidal flats in North Jiangsu Province. *Journal of Geographical Sciences*, *20*, 91–108.

Liu, Z., Pan, S., Yin, Y., Ma, R., Gao, J., Xia, F., & Yang, X. (2013). Reconstruction of the historical deposition environment from ^{210}Pb and ^{137}Cs records at two tidal flats in China. *Ecological Engineering*, *61*, 303–315.

Liu, Z. Y., Pan, S. M., Yin, Y., Huang, J. X., Wang, A. D., & Pang, R. S. (2010). Depositional environment and distribution characteristics of heavy metals in Linhong estuary. *Geochimica*, *39*(5), 456–468. (in Chinese).

Loh, P. S., Cheng, L., Yuan, H., Yang, L., Lou, Z., Jin, A., & Chen, C. A. (2018). Impacts of human activity and extreme weather events on sedimentary organic matter in the Andong salt marsh, Hangzhou Bay, China. *Continental Shelf Research*, *154*, 55–64.

Long, M. L. (2018). The impact of invasive smooth cordgrass (*Spartina alterniflora* Loisel.) on organic carbon stock in Jiuduansha wetland. Shanghai University (in Chinese).

Lu, W., Liu, C., Zhang, Y., Yu, C., Cong, P., Ma, J., & Xiao, J. (2019). Carbon fluxes and stocks in a carbonate-rich chenier plain. *Agricultural and Forest Meteorology*, *275*, 159–169.

Lu, W., Yang, S. Y., Chen, L., Wang, W., Du, X., Wang, C., & Lin, G. (2014). Changes in carbon pool and stand structure of a native subtropical mangrove forest after inter-planting with exotic species *Sonneratia apetala*. *PLoS One*, *9*, e91238.

Lunstrum, A., & Chen, L. (2014). Soil carbon stocks and accumulation in young mangrove forests. *Soil Biology & Biochemistry*, *75*, 223–232.

Luo, X., Zhang, S., & Dun, M. (2010). Spatial distribution and seasonal dynamics characteristics of carbon, nitrogen and phosphorus in the Liaohe Estuary wetlands. *Periodical of Ocean University of China*, *40*, 97–104. (in Chinese).

Ma, C., Lin, T., Ye, S., Ding, X., Li, Y., & Guo, Z. (2017). Sediment record of polycyclic aromatic hydrocarbons in the Liaohe River Delta wetland, Northeast China: Implications for regional population migration and economic development. *Environmental Pollution*, *222*, 146–152.

Mao, Z., Lai, D., Zhao, Z., & Yang, X. (2014). Effect of invasion plants (*Mikania micrantha* H.B.K.) on carbon stock of mangrove ecosystem in Shenzhen Bay. *Ecology and Environmental Sciences*, *75*, 223–232. (in Chinese).

Meng, X., Xia, P., Li, Z., & Meng, D. (2016). Mangrove degradation and response to anthropogenic disturbance in the Maowei Sea (SW China) since 1926 AD: Mangrove-derived OM and pollen. *Organic Geochemistry*, *98*, 166–175.

Mo, L. P., Zhou, H. J., Liu, Y. D., Li, Q. Y., & Liang, X. H. (2015). An estimation of soil organic carbon storage in mangrove wetlands of Guangxi. *Journal of Anhui Agricultural Science*, *43*(15), 81–84. (in Chinese).

Pan, S. M., Tims, S. G., Liu, X. Y., & Fifield, L. K. (2011). ^{137}Cs, $^{239+240}$Pu concentrations and the ^{240}Pu/^{239}Pu atom ratio in a sediment core from the sub-aqueous delta of Yangtze River estuary. *Journal of Environmental Radioactivity*, *102*, 930–936.

Pang, R. S., Pan, S. M., & Wang, A. D. (2011). Modern sedimentation rate and its implications for environmental evolutions of 18# core in the Changjiang estuary in China. *Marine Science Bulletin*, *30*(3), 294–301. (in Chinese).

Qiao, Y. M., Tan, J. B., Ma, S. X., Zhao, J. G., Wu, Y. L., & Du, H. (2018). The distribution pattern and sources analysis for nitrogen and phosphorus in core sediment of Shenzhen mangrove wetland. *Environmental Science & Technology*, *41*(2), 34–40. (in Chinese).

Song, H. L., Liu, X. T., Wang, L. Z., Yu, W. N., & Dong, B. (2018). Spatial and temporal distribution of soil organic carbon in vegetation communities of the Yellow River Delta under different disturbance level. *Journal of Soil and Water Conservation*, *32*(1), 190–203 (in Chinese).

Su, Z., Qiu, G., Fan, H., Li, M., & Fang, C. (2020). Changes in carbon storage and macrobenthic communities in a mangrove-seagrass ecosystem after the invasion of smooth cordgrass in southern China. *Marine Pollution Bulletin*, *152*, 110887.

Sun, H., Jiang, J., Cui, L., Zhang, S., & Zhang, J. (2018). Effects of *Spartina alterniflora* invasion on soil organic carbon composition of mangrove wetland in Zhangjiang River estuary. *Chinese Journal of Plant Ecology*, *42*, 774–784. (in Chinese).

Tan, L. S., Ge, Z. M., Fei, B. L., Xie, L. N., & Li, Y. L. (2020). The roles of vegetation, tide and sediment in the variability of carbon in the salt marsh dominated tidal creeks. *Estuarine, Coastal and Shelf Science*, *239*, 106752.

Tao, Y., Huang, X., Wang, X., & Zhong, Q. (2020). Soil carbon and nitrogen storages in three mangrove stands of Zhenzhu Gulf, Guangxi. *Guihaia*, *40*, 285–292. (in Chinese).

Tao, Y., Huang, X., Wang, X., Zhong, Q., & Kang, Z. (2020). Spatial distribution of soil carbon and nitrogen stocks in mangrove wetland of Xiandao Park and Shajing, Guangxi. *Progress in Fishery Sciences*, *41*(5), 38–45. (in Chinese).

Wan, S., Liu, X., & Mu, X. (2017). Vertical distribution characteristics of carbon and nitrogen contents in soils of 4 types of wetlands in Shuangtai River estuary. *Wetland Science*, *15*, 629–634. (in Chinese).

Wang, D., Zhang, R., Xiong, J., Guo, H., & Zhao, B. (2015). Contribution of invasive species *Spartina alterniflora* to soil organic carbon pool in coastal wetland: Stable isotope approach. *Chinese Journal of Plant Ecology*, *39*, 941–949. (in Chinese).

Wang, G., Guan, D., Peart, M. R., Chen, Y., & Peng, Y. (2013). Ecosystem carbon stocks of mangrove forest in Yingluo Bay, Guangdong Province of South China. *Forest Ecology and Management*, *310*, 539–546.

Wang, G., Guan, D., Xiao, L., & Peart, M. R. (2019). Ecosystem carbon storage affected by intertidal locations and climatic factors in three estuarine mangrove forests of South China. *Regional Environmental Change*, *19*, 1701–1712.

Wang, H., Sun, Z., Li, J., He, T., Gao, H., Wang, J., & Wu, X. (2018). Spatial variations of soil carbon and nitrogen contents in *Phragmites australis* and *Cyperus malaccensis* marsh in the Minjiang River estuary. *Chinese Journal of Ecology*, *37*, 1102–1110. (in Chinese).

Wang, H. J., He, Z. Z., Hu, J. J., He, X. W., Peng, C., & Guan, Y. J. (2017). Sedimentation rates in Guangxi Beibu gulf. *Journal of Guangxi University (Natural Science Edition)*, *42*(6), 2120–2126. (in Chinese).

Wang, Q., Song, J., Cao, L., Li, X., Yuan, H., & Li, N. (2017). Distribution and storage of soil organic carbon in a coastal wetland under the pressure of human activities. *Journal of Soils and Sediments*, *17*, 11–22.

Wang, Q., Song, J., Li, X., Yuan, H., Li, N., & Cao, L. (2016). Environmental evolution records reflected by radionuclides in the sediment of coastal wetlands: A case study in the Yellow River Estuary wetland. *Journal of Environmental Radioactivity*, *162*, 87–96.

Wang, W., Wang, C., Sardans, J., Tong, C., Jia, R., Zeng, C., & Penuelas, J. (2015). Flood regime affects soil stoichiometry and the distribution of the invasive plants in subtropical estuarine wetlands in China. *Catena*, *128*, 144–154.

Wu, M., He, Z., Fung, S., Cao, Y., Guan, D., Peng, Y., & Lee, S. Y. (2020). Species choice in mangrove reforestation may influence the quantity and quality of long-term carbon sequestration and storage. *Science of the Total Environment*, *714*, 136742.

Wu, Q., Leung, J. Y., Tam, N. F., Chen, S., Mai, B., Zhou, X., & Geng, X. (2014). Biological risk and pollution history of polycyclic aromatic hydrocarbons (PAHs) in Nansha mangrove, South China. *Marine Pollution Bulletin*, *85*, 92–98.

Xia, P., Meng, X., Li, Z., & Feng, A. (2017). Organic carbon isotope and pollen evidence for mangrove development and response to human activity in Guangxi (Southwest China) over the last 140 years. *Acta Oceanologica Sinica*, *36*, 11–21.

Xia, P., Meng, X., Li, Z., Feng, A., Yin, P., & Zhang, Y. (2015). Mangrove development and its response to environmental change in Yingluo Bay (SW China) during the last 150 years: Stable carbon isotopes and mangrove pollen. *Organic Geochemistry*, *85*, 32–41.

Xia, P., Meng, X. W., Feng, A. P., Li, Z., & Yang, G. (2015). Sediment compaction rates in mangrove swamps of Guangxi and its mangrove migration response to sea-level rise. *Acta Sedimentologica Sinica*, *33*(3), 551–560. (in Chinese).

Xia, P., Meng, X. W., Li, Z., Feng, A. P., & Wang, X. Q. (2012). Sedimentary records of environmental evolution during the recent 100 years in the coastal zone of Guangxi province. *Acta Sedimentologica Sinica*, *30*(2), 325–332. (in Chinese).

Xie, W., Zhu, K., Cui, Y., Du, H., & Chen, J. (2014). Spatial distribution of soil carbon and nitrogen in Jiaozhou Bay estuarine wetland. *Acta Prataculturae Sinica*, *23*, 54–60. (in Chinese).

Xin, K., Yan, K., Li, Z., Hu, J., & Qiu, M. (2014). Distribution of soil organic carbon in mangrove wetlands of Hainan Island and its influencing factors. *Acta Pedologica Sinica*, *51*, 1078–1086. (in Chinese).

Xiong, Y., Liao, B., Proffitt, E., Guan, W., Sun, Y., Wang, F., & Liu, X. (2018a). Soil carbon storage in mangroves is primarily controlled by soil properties: A study at Dongzhai Bay, China. *Science of the Total Environment*, *619*, 1226–1235.

Xiong, Y., Liao, B., & Wang, F. (2018b). Mangrove vegetation enhances soil carbon storage primarily through in situ inputs rather than increasing allochthonous sediments. *Marine Pollution Bulletin*, *131*, 378–385.

Xu, Y. W., Jiang, Z. M., Wu, F., Yang, Q. L., & Liao, B. W. (2020). Soil organic carbon distribution and its correlation with soil physical and chemical indexes of *Sonneratia apetala* plantation at Cuiheng wetland. *Forest Research*, *33*(1), 62–68. (in Chinese).

Yan, G., Ge, Z. M., & Zhang, L. Q. (2014). Distribution of soil carbon storage in different saltmarsh plant communities in Chongming Dongtan wetland. *Chinese Journal of Applied Ecology*, *25*(1), 85–91. (in Chinese).

Yan, J., He, D., Li, X., Wang, R., Cai, J., You, W., & Xiao, S. (2013). Comparative studies on the carbon storage between the *Kandelia candel* natural forests and plantations in north mangrove forests of China. *Chinese Journal of Tropical Crops*, *34*, 1395–1401. (In Chinese).

Yang, B., Wang, F., Tian, L. Z., Chen, Y. S., Jiang, X. Y., Wang, H., Hu, K., Fang, J., Li, J. F., & Shang, Z. W. (2016). Deposition of modern flooding events indicated by $^{210}Pb_{exc}$ and ^{137}Cs records from salt marsh of the Duliujian River, Tianjin. *Journal of Marine Sciences*, *34*(2), 10–18. (in Chinese).

Yang, J., Gao, J., Liu, B., & Zhang, W. (2014). Sediment deposits and organic carbon sequestration along mangrove coasts of the Leizhou Peninsula, southern China. *Estuarine, Coastal and Shelf Science*, *136*, 3–10.

Yang, J., Gao, J., Liu, B. L., Cheung, A., Wang, L., & Zhang, W. (2012). Edge effects of mangrove boundaries and their impact in organic carbon pool along the coast of Leizhou Peninsula. *Acta Oceanologica Sinica*, *34*(5), 161–168 (in Chinese).

Yang, M. L., Gao, T. W., Xing, Y. Z., Lu, Y. Z., Nong, Y., & Liu, W. A. (2017). Study on the food sources of mangrove macrobenthos in Liaozhou, Bay. *Guangxi Sciences*, *24*(5), 490–497. (in Chinese).

Yang, R. (2019). Interacting effects of plant invasion, climate, and soils on soil organic carbon storage in coastal wetlands. *Journal of Geophysical Research: Biogeosciences*, *124*, 2554–2564.

Yang, T., Ren, H., Zhang, Z., Chen, Y., & Jiang, D. (2016). Distribution and influence factors of soil organic carbon of different land-use types in the Jiangsu coastal areas. *Journal of Subtropical Resources and Environment*, *11*, 46–52. (in Chinese).

Ye, S., Laws, E. A., Yuknis, N., Ding, X., Yuan, H., Zhao, G., & Delaune, R. D. (2015). Carbon sequestration and soil accretion in coastal wetland communities of the Yellow River Delta and Liaohe Delta, China. *Estuaries and Coasts*, *38*, 1885–1897.

Ye, X., Wang, A., & Chen, J. (2014). Distribution and deposition characteristics of carbon and nitrogen in sediments in a semi-closed bay area, Southeast China. *Continental Shelf Research*, *90*, 133–141.

Yu, C., Feng, J., Liu, K., Wang, G., Zhu, Y., Chen, H., & Guan, D. (2020). Changes of ecosystem carbon stock following the plantation of exotic mangrove *Sonneratia apetala* in Qi'ao Island, China. *Science of the Total Environment*, *717*, 137142.

Yu, C., Guan, D., Wang, G., Lou, D., & Feng, J. (2021). Development of ecosystem carbon stock with the progression of a natural mangrove forest in Yingluo Bay, China. *Plant and Soil*, *460*(1–2), 391–401.

Yu, J., Dong, H., Li, Y., Wu, H., Guan, B., Gao, Y., & Wang, Y. (2014). Spatiotemporal distribution characteristics of soil organic carbon in newborn coastal wetlands of the Yellow River Delta Estuary. *Clean-Soil Air Water*, *42*, 311–318.

Zang, Z. (2019). Analysis of intrinsic value and estimating losses of "blue carbon" in coastal wetlands: A case study of Yancheng, China. *Ecosystem Health and Sustainability*, *5*, 216–225.

Zhang, D., Yan, D., Jiang, X., Lin, X., Liu, N., Liu, K., & Yin, P. (2018). Influence of anthropogenic activities on polycyclic aromatic hydrocarbons in sediments from mangrove wetland at Dongzhai Harbor, China: Distribution, sources,

probability risk, and temporal trend. *Wetlands Ecology and Management*, *26*, 613–625.
Zhang, H. B., Kong, F. L., Xi, M., Li, Y., & Sun, X. L. (2018). Responses of soil labile organic carbon and enzyme activity to *Spartina alterniflora* invasion in estuary wetland of Jiaozhou Bay. *Acta Ecologica Sinica*, *38*(13), 4869–4878. (in Chinese).
Zhang, H. Y. (2014). Yangtze estuary typical tidal wetlands—Chongxi wetland soil organic carbon distribution and research of ecological engineering influence. East China Normal University (in Chinese).
Zhang, P. (2016). Sedimentary environment changes and events response of Liao River estuary entrance shoal in nearly 50 years. China University of Geosciences (Beijing) (in Chinese).
Zhang, W. M. (2016). *Distribution characteristics and spatial heterogeneity of soil organic carbon on the south coast of Hangzhou Bay*. Nanjin Agricultural University (in Chinese).
Zhang, X. L., Shi, S. L., Pan, G. X., Li, L. Q., Zhang, X. H., & Li, Z. P. (2008). Changes in eco-chemical properties of a mangrove wetland under *Spartina alterniflora* from Zhangjiang Kou, Fujian, China. *Advances in Earth Science*, *9*, 974–981. (in Chinese).
Zhang, Y., Du, J., Zhao, X., Wu, W., Peng, B., & Zhang, J. (2014). A multi-proxy study of sedimentary humic substances in the salt marsh of the Changjiang Estuary, China. *Estuarine, Coastal and Shelf Science*, *151*, 295–301.
Zhang, Y., Meng, X., Xia, P., Zhang, J., & Wang, W. (2021). Spatiotemporal variations in the organic carbon accumulation rate in mangrove sediments from the Yingluo bay, China, since 1900. *Acta Oceanologica Sinica*, *40*(8), 65–77.
Zhang, Y. F., Zhang, Z. K., Meng, H. M., Zhang, L. H., & Yu, K. F. (2012). Geochemical evidences of the land subsidence induced by the historical earthquake in 1605, Hainan Island, China. *Quaternary Sciences*, *32*(6), 1248–1254. (in Chinese).
Zhang, Z., Wang, Y., Zhu, Y., He, K., Li, T., Mishra, U., & Qin, Z. (2022). Carbon sequestration in soil and biomass under native and non-native mangrove ecosystems. *Plant and Soil*, *479*, 1–16.
Zhao, Q., Bai, J., Liu, P., Gao, H., & Wang, J. (2015). Decomposition and carbon and nitrogen dynamics of phragmites australis litter as affected by flooding periods in coastal wetlands. *Clean Soil Air Water*, *43*(3), 441–445.
Zhao, Z., Zhuang, Y., & Gu, J. D. (2012). Abundance, composition and vertical distribution of polycyclic aromatic hydrocarbons in sediments of the Mai Po Inner Deep Bay of Hong Kong. *Ecotoxicology*, *21*, 1734–1742.
Zhou, H. J., Mo, L. P., Liu, Y. D., Li, Q. Y., & Liang, Y. (2015). Correlation analysis between soil organic carbon density and soil physical and chemical properties of mangrove wetland in Qinzhou Bay of Guangxi. *Journal of Anhui Agricultural Science*, *43*(17), 120–123 (in Chinese).
Zhu, Y., Zhao, F., Guo, J., Wu, G., & Lin, G. (2016). Below-ground organic carbon distribution and burial characteristics of the Gaoqiao mangrove area in Zhanjiang, Guangdong, Southern China. *Acta Ecologica Sinica*, *36*, 7841–7849. (in Chinese).
Zi, Y., Xi, M., Kong, F., Li, Y., & Yang, L. (2016). Temporal and spatial distribution of soil organic carbon and its storage in the coastal wetlands of Jiaozhou Bay, China. *Chinese Journal of Applied Ecology*, *27*, 2075–2083. (in Chinese).

SUPPORTING INFORMATION

Additional supporting information can be found online in the Supporting Information section at the end of this article.

How to cite this article: Fan, B., & Li, Y. (2024). China's conservation and restoration of coastal wetlands offset much of the reclamation-induced blue carbon losses. *Global Change Biology*, *30*, e17039. https://doi.org/10.1111/gcb.17039